

First order radiative corrections to Bhabha scattering in d dimensions ^{*}

J. Fleischer¹, J. Gluza², A. Lorca^{3,4} and T. Riemann⁴ [†]

¹ Fakultät für Physik, Universität Bielefeld, Universitätsstr. 25, 33615 Bielefeld, Germany

² Department of Field Theory and Particle Physics, Institute of Physics, University of Silesia,
Uniwersytecka 4, 40007 Katowice, Poland

³ Physikalisches Institut, Albert-Ludwigs-Universität Freiburg, Hermann-Herder-Str. 3, 79104
Freiburg, Germany

⁴ Deutsches Elektronen-Synchrotron, DESY, Platanenallee 6, 15738 Zeuthen, Germany

Abstract

The luminosity measurement at the projected International Linear e^+e^- Collider ILC is planned to be performed with forward Bhabha scattering with an accuracy of the order of 10^{-4} . A theoretical prediction of the differential cross-section has to include one-loop weak corrections, with leading higher order terms, and the complete two-loop QED corrections. Here, we present the weak part and the virtual one-loop photonic corrections. For the photonic corrections, the expansions in $\epsilon = (4 - d)/2$ are derived with inclusion of the terms of order ϵ in order to match the two-loop accuracy. For the photonic box master integral in d dimensions we compare several different methods of evaluation.

^{*}Work supported in part by the European Community's Human Potential Programme under contract HPRN-CT-2000-00149 'Physics at Colliders' and by Sonderforschungsbereich/Transregio 9 of DFG 'Computergestützte Theoretische Teilchenphysik'.

[†]E-mails: fleischer@physik.uni-bielefeld.de, Janusz.Gluza@desy.de, Alejandro.Lorca@physik.uni-freiburg.de, Tord.Riemann@desy.de

1 Introduction

Bhabha scattering

$$e^-(p_1) + e^+(p_4) \rightarrow e^-(-p_2) + e^+(-p_3) \quad (1.1)$$

was one of the first processes calculated in quantum theory [1]. The complete virtual electroweak one-loop corrections have been first calculated in [2], later also in [3–11]. By now, Bhabha scattering may also be calculated with automated tools for the evaluation of Feynman diagrams and cross-sections as e.g. `Feynarts` [12, 13], `grace` [14] and `aITALC` [15]. The electroweak corrections have to be considered together with hard bremsstrahlung corrections, which usually are calculated by Monte Carlo programs; see [16–20] and references therein. Dedicated studies for experimentation at LEP may be found in [21, 22] and references therein.

The preparation of the e^+e^- linear collider project ILC (formerly also TESLA [23], and corresponding projects of other regions) triggered again some interest in both wide angle and small angle Bhabha scattering. The latter might allow to determine the luminosity with an unprecedented accuracy of 10^{-4} . For this, one needs theoretical predictions beyond one-loop accuracy in the extreme forward scattering region where the cross-section peaks due to the kinematical singularity of the photon propagators, while the pure weak corrections might be sufficient in one-loop approximation (with leading higher order terms *à la* [7]). If a so-called Giga-Z option will be realized, high Bhabha event rates are to be expected in the Z resonance region also for larger scattering angles.

We write the matrix element squared

$$\begin{aligned} |\mathcal{M}|^2 &= (\mathcal{M}^{(0)} + \mathcal{M}^{(1)} + \dots)^* (\mathcal{M}^{(0)} + \mathcal{M}^{(1)} + \dots) + (\mathcal{M}_\gamma^{(0)} + \dots)^* (\mathcal{M}_\gamma^{(0)} + \dots) + \dots \\ &= \underbrace{|\mathcal{M}^{(0)}|^2}_{\mathcal{O}(\alpha^2)} + \underbrace{2\Re(\mathcal{M}^{(0)*}\mathcal{M}^{(1)}) + |\mathcal{M}_\gamma^{(0)}|^2}_{\mathcal{O}(\alpha^3)} \\ &\quad + \underbrace{|\mathcal{M}^{(1)}|^2 + 2\Re(\mathcal{M}^{(0)*}\mathcal{M}^{(2)}) + 2\Re(\mathcal{M}_\gamma^{(0)*}\mathcal{M}_\gamma^{(1)}) + |\mathcal{M}_{\gamma\gamma}^{(0)}|^2}_{\mathcal{O}(\alpha^4)} + \mathcal{O}(\alpha^5), \end{aligned} \quad (1.2)$$

where $\mathcal{M}^{(i)}$ is the contribution to the i -loop order and the subscripts γ and $\gamma\gamma$ indicate the emission of one or two photons.

The QED contributions dominate by far and two-loop corrections are also needed. Several projects to determine them in a systematic way are underway (see [24–29] and references therein). A program with two-loop accuracy has to include also the complete one-loop matrix elements squared, often regulated by an expansion in $\epsilon = (d - 4)/2$, with a careful treatment of the resulting finite terms in ϵ .¹ For this, one may express the Feynman diagrams by scalar master integrals, which then have to be known up to some positive order in ϵ . Thus, one has to go beyond the usual technical demands of a pure one-loop calculation.

In this article, we give a concise description of our approach to the one-loop contributions for a two-loop calculation of massive Bhabha scattering. Introductory, we present in Section 2

¹A similar program was performed in [30, 31].

electroweak predictions which were obtained for the ILC study [23, 32, 33]. The expressions for the pure QED corrections up to order ϵ in terms of a few scalar master integrals are derived in Section 3. Here we retain the exact dependences on the electron mass. The scalar master integrals are discussed in Section 4. For the box master integral we compare several, quite different expressions, which are derived with the aid of a difference equation, a system of differential equations, and the Mellin-Barnes technique, respectively. We close with a short Summary.

2 Electroweak one-loop corrections

One-loop corrections are the virtual part of the $\mathcal{O}(\alpha^3)$ terms in (1.2). The calculation of electroweak corrections to Bhabha scattering with the automated tool `aITALC` has been described on several occasions [15, 32–35]. `aITALC` [15] uses the packages `DIANA v.2.35/QGRAF 2` [36, 37] for the creation of the one-loop matrix elements, `FORM 3.1` [38] for their expressions in terms of scalar `s`, and `LoopTools 2.1/FF` [39, 40] for the numerical evaluation, including also soft bremsstrahlung. In one respect we had to go beyond `LoopTools 2.1`: In order to evaluate cross-sections in the neighbourhood of the Z resonance peak, one has to use Breit-Wigner propagators in the s -channel, replacing m_Z^2 by $m_0^2 = m_Z^2 - im_Z \Gamma_Z$. Accordingly, the γZ box function $D_0(t, s, m_0) = D_0(m^2, m^2, m^2, m^2, t, s, \lambda^2, m^2, m_0^2, m^2)$, if used with (γ, Z) in the s -channel, has been modified as in [41]:

$$D_0(t, s, m_0) = \frac{x_s}{m_1 m_4 (t - m_0^2) (1 - x_s^2)} \left\{ \begin{aligned} &+ 2 \log(x_s) \left(\log(1 - x_s^2) - \log \frac{m_0 \lambda}{m_0^2 - t - i\epsilon} \right) \\ &+ \frac{\pi^2}{2} + \text{Li}(x_s^2) + \log^2(x_2) + \log^2(x_3) \\ &- \sum_{\sigma, \rho = \pm 1} (\text{Li}(x_s x_2^\rho x_3^\sigma) + (\log x_s + \log x_2^\rho + \log x_3^\sigma) \log(1 - x_s x_3^\sigma x_2^\rho)) \end{aligned} \right\} \quad (2.1)$$

The diagram is shown in Figure 2.1.

We use the `LoopTools` conventions $s = (p_1 + p_4)^2$, $t = (p_1 + p_2)^2$, $p_i^2 = m_i^2 = m^2$, $\lambda = m_\gamma$, with the following definitions for the x variables

$$x_s \equiv -K(s + i\epsilon, m_1, m_4), \quad (2.2)$$

$$x_2 \equiv -K(m_2^2, m_1, m_0), \quad (2.3)$$

$$x_3 \equiv -K(m_3^2, m_4, m_0), \quad (2.4)$$

and the definition of the K -function (with one of the arguments being complex)

$$K(z, m, m') \equiv \begin{cases} \frac{1 - \sqrt{1 - \frac{4mm'}{z - (m - m')^2}}}{1 + \sqrt{1 - \frac{4mm'}{z - (m - m')^2}}} & z \neq (m - m')^2, \\ -1 & z = (m - m')^2. \end{cases} \quad (2.5)$$

$\cos \theta$	Born EWSM	$\mathcal{O}(\alpha)$ EWSM
-0.9	$0.12201 \cdot 10^4$	$0.11767 \cdot 10^4$
-0.7	$0.10099 \cdot 10^4$	$0.95012 \cdot 10^3$
-0.5	$0.85685 \cdot 10^3$	$0.79246 \cdot 10^3$
0	$0.73164 \cdot 10^3$	$0.64561 \cdot 10^3$
+0.5	$0.10701 \cdot 10^4$	$0.91360 \cdot 10^3$
+0.7	$0.16162 \cdot 10^4$	$0.13917 \cdot 10^4$
+0.9	$0.70112 \cdot 10^4$	$0.63472 \cdot 10^4$
+0.99	$0.62198 \cdot 10^6$	$0.57186 \cdot 10^6$
+0.999	$0.62612 \cdot 10^8$	$0.57540 \cdot 10^8$
+0.9999	$0.62666 \cdot 10^{10}$	$0.57822 \cdot 10^{10}$

Table 2.1: Differential cross-sections in pbarn for Bhabha scattering at $\sqrt{s} = m_Z$. Born contribution and the $\mathcal{O}(\alpha)$ correction are shown; the maximum soft-photon energy is $\sqrt{s}/10$.

The photon mass is λ in `LoopTools`. The use of this scalar box function is not only necessary in order to regulate the γZ box contribution, but also for a proper compensation of the corresponding soft photon infra-red divergencies which are proportional to the Born cross-section with a Breit-Wigner Z propagator. The implementation is done in the file `fortran/src/d0wdd0.F` of the `aITALC` package.

In Tables 2.1 and 2.2 we provide numerical sample outputs at typical energies for several scattering angles. The input quantities as well as the treatment of soft photons are exactly the same as in [42]. The cross-section peak in the forward direction, due to the photon exchange in the t -channel. In this kinematic region, the pure photonic corrections will be dominating and we have to treat them with higher accuracy than the rest of the electroweak corrections. For the one-loop corrections, this means a determination of $|\mathcal{M}^{(1)}|^2$ as part of the $\mathcal{O}(\alpha^4)$ terms in (1.2). Here one needs the QED one-loop functions including terms of order ϵ because their interference with other terms of order $1/\epsilon$ contributes to the finite cross-section. This will be the main concern of the rest of this article.

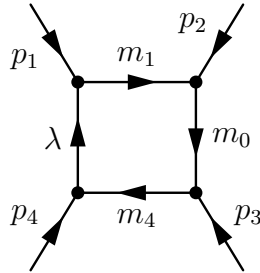


Figure 2.1: Four-point function with complex mass m_0 and photon mass regulator λ .

rad	$\cos \theta$	Born EWSM	$\mathcal{O}(\alpha)$ EWSM		$\mathcal{O}(\alpha)$ QED $N_f = 9$	
2.691	-0.9	$2.16999 \cdot 10^{-1}$	$1.93445 \cdot 10^{-1}$	-10.85%	$4.69800 \cdot 10^{-1}$	116.50%
2.346	-0.7	$2.30098 \cdot 10^{-1}$	$2.08843 \cdot 10^{-1}$	-9.24%	$5.03879 \cdot 10^{-1}$	118.98%
2.094	-0.5	$2.61360 \cdot 10^{-1}$	$2.38707 \cdot 10^{-1}$	-8.67%	$5.66238 \cdot 10^{-1}$	116.65%
1.571	0	$5.98142 \cdot 10^{-1}$	$5.46677 \cdot 10^{-1}$	-8.60%	$1.09322 \cdot 10^0$	82.77%
1.047	+0.5	$4.21273 \cdot 10^0$	$3.81301 \cdot 10^0$	-9.49%	$5.13530 \cdot 10^0$	21.90%
0.795	+0.7	$1.58240 \cdot 10^1$	$1.43357 \cdot 10^1$	-9.41%	$1.64548 \cdot 10^1$	3.99%
0.451	+0.9	$1.89160 \cdot 10^2$	$1.72928 \cdot 10^2$	-8.58%	$1.76464 \cdot 10^2$	-6.71%
0.142	+0.99	$2.06556 \cdot 10^4$	$1.90607 \cdot 10^4$	-7.72%	$1.91774 \cdot 10^4$	-7.16%
0.045	+0.999	$2.08236 \cdot 10^6$	$1.91624 \cdot 10^6$	-7.98%	$1.92546 \cdot 10^6$	-7.53%
0.014	+0.9999	$2.08429 \cdot 10^8$	$1.91402 \cdot 10^8$	-8.17%	$1.92270 \cdot 10^8$	-7.75%

Table 2.2: Differential cross-sections in pbarn for Bhabha scattering at $\sqrt{s} = 500$. Born contribution, the $\mathcal{O}(\alpha)$ correction, and also a QED prediction are shown; the maximum soft-photon energy is $\sqrt{s}/10$.

3 The massive QED cross-section in d dimensions

The ten diagrams of Fig. (3.1) are the one-loop contributions in pure QED.

We decompose the full one-loop matrix element as follows:

$$\begin{aligned}
\mathcal{M}_1 &= [\gamma_\mu \otimes \gamma_\mu] F_1, \\
\mathcal{M}_2 &= [\not{p}_4 \otimes \not{p}_2] F_2, \\
\mathcal{M}_3 &= [\gamma_\mu \gamma_\nu \gamma_\rho \otimes \gamma_\rho \gamma_\nu \gamma_\mu] F_3, \\
\mathcal{M}_4 &= [\gamma_\mu \gamma_\nu \not{p}_4 \otimes \gamma_\nu \gamma_\mu \not{p}_2] F_4, \\
\mathcal{M}_5 &= ([\not{p}_4 \otimes 1] + [1 \otimes \not{p}_2]) F_5, \\
\mathcal{M}_6 &= ([\gamma_\mu \not{p}_4 \otimes \gamma_\mu] + [\gamma_\mu \otimes \gamma_\mu \not{p}_2]) F_6, \\
\mathcal{M}_7 &= [1 \otimes 1] F_7, \\
\mathcal{M}_8 &= [\gamma_\mu \gamma_\nu \otimes \gamma_\nu \gamma_\mu] F_8, \\
\mathcal{M}_9 &= ([\gamma_\mu \gamma_\nu \not{p}_4 \otimes \gamma_\nu \gamma_\mu] + [\gamma_\mu \gamma_\nu \otimes \gamma_\nu \gamma_\mu \not{p}_2]) F_9.
\end{aligned} \tag{3.1}$$

The notation is short-hand for the s and t channel matrix elements:

$$\begin{aligned}
\mathcal{M}_k^{(s)} &= O_i \otimes O_f F_k(s, t) \\
&= \bar{v}(p_4) O_i u(p_1) \cdot \bar{u}(-p_2) O_f v(-p_3) F_k(s, t),
\end{aligned} \tag{3.2}$$

$$\begin{aligned}
\mathcal{M}_k^{(t)} &= O_e \otimes O_p [-F_k(t, s)] \\
&= \bar{v}(p_4) O_e v(-p_3) \cdot \bar{u}(-p_2) O_p u(p_1) [-F_k(t, s)].
\end{aligned} \tag{3.3}$$

Crossing the diagrams from the s -channel to the t -channel results in the exchange of s and t and in an overall sign change due to Fermi statistics; see Equation (3.3). In general the first six

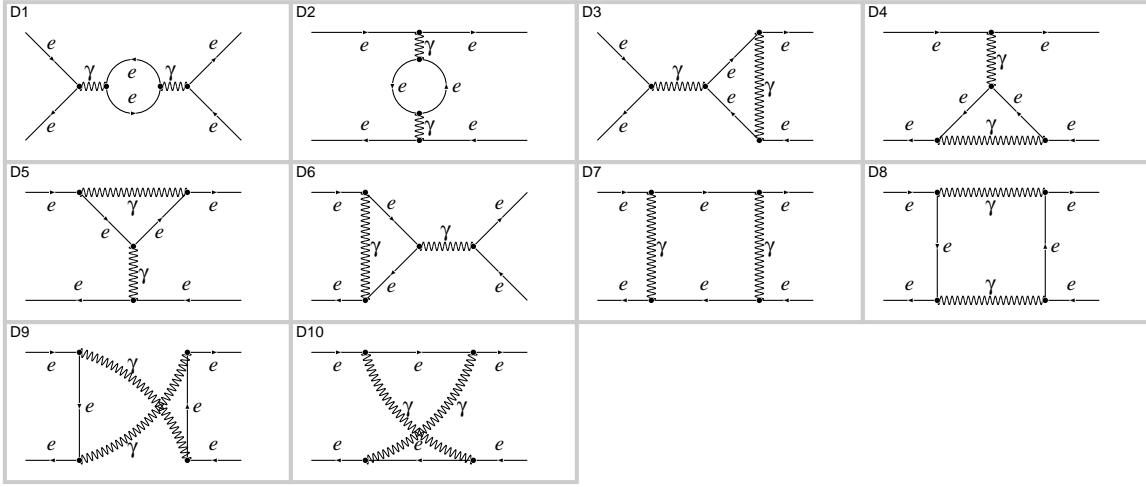


Figure 3.1: One-loop diagrams for the process $e^+e^- \rightarrow e^+e^-$.

amplitudes are independent while F_7 to F_9 can be expressed in terms of them, but in slightly different ways for the various cases under consideration. For this reason we list them all.

With the form factors $F_k(s, t)$ one may determine the contributions from $2\Re(\mathcal{M}^{(0)*}\mathcal{M}^{(1)})$ and from $|\mathcal{M}^{(1)}|^2$ to the differential cross-section (1.2). The interference of $\mathcal{M}^{(0)}$ and $\mathcal{M}^{(1)}$ yields e.g.:

$$\frac{d\sigma}{d\cos\theta} = \frac{\pi\alpha^2}{2s} \sum_{j=1}^9 [B_j(s, t)F_j(s, t) + B_j(t, s)F_j(t, s)], \quad (3.4)$$

with

$$\begin{aligned} B_1 &= s \left\{ 4(1+v)^2 + 2(1-v + \frac{1}{v}) - 4vz^2 + (1 - \frac{1}{2v})z^4 \right\}, \\ B_2 &= s^2 \left\{ -(1+v)[(1+v)^2 + v^2] + \frac{1}{2}[(1+v)^2 + v(3+5v) - \frac{1}{2v}]z^2 - \right. \\ &\quad \left. \frac{3}{4}(2v - \frac{1}{2v})z^4 + \frac{1}{4}(1 - \frac{1}{2v})z^6 \right\}, \\ B_3 &= s \left\{ 8(3+3v+5v^2) + \frac{8}{v} + 8(3-5v + \frac{3}{v})z^2 + 2(5 - \frac{7}{v})z^4 \right\}, \\ B_4 &= s^2 \left\{ -4(1+v)v^2 - (2-6v^2 + \frac{1}{v})z^2 + (3-4v + \frac{3}{v})z^4 + (1 - \frac{5}{4v})z^6 \right\}, \\ B_5 &= ms \left\{ -2(6v+4v^2 - \frac{1}{v}) + (2+8v - \frac{3}{v})z^2 - (2 - \frac{1}{v})z^4 \right\}, \\ B_6 &= ms \left\{ -4(3 + \frac{1}{v}) + 2(1+2v)z^2 - (2 - \frac{1}{v})z^4 \right\}, \end{aligned}$$

$$\begin{aligned}
B_7 &= s \left\{ -\frac{1}{v} - 2\left[1 + v - \frac{3}{4v}\right]z^2 + \left(1 - \frac{1}{2v}\right)z^4 \right\}, \\
B_8 &= s \left\{ -\frac{4}{v} + 4\left(1 - 2v + \frac{3}{v}\right)z^2 + \left(4 - \frac{5}{v}\right)z^4 \right\}, \\
B_9 &= ms \left\{ -8\left(3v + 4v^2 - \frac{1}{v}\right) - 4\left(3 - 8v + \frac{6}{v}\right)z^2 - 2\left(4 - \frac{5}{v}\right)z^4 \right\},
\end{aligned} \tag{3.5}$$

and

$$v = \frac{t}{s}, \tag{3.6}$$

$$z = \frac{4m^2}{s}. \tag{3.7}$$

With the same formula (3.4), the Born cross-section, arising from $|\mathcal{M}^{(0)}|^2$, is obtained with:

$$F_1^{Born}(s, t) = \frac{1}{s}, \tag{3.8}$$

$$F_j^{Born}(s, t) = 0 \text{ for } j > 1. \tag{3.9}$$

The contributions from $|\mathcal{M}^{(1)}|^2$ to the cross-section are rather lengthy and not shown here explicitly; they will be provided on the webpage [43]. There we give also the expressions for the corresponding interferences in d dimensions.

Before determining the form factors $F_k(s, t)$, we discuss now the various contributions. As mentioned we may restrict ourselves to the s -channel diagrams D1, D3, D6, D8, D9:

$$F_j(s, t) = \frac{2e^2}{(4\pi)^{d/2}} \left(F_j^{self} + F_j^{vert} + F_j^{box} \right), \quad j = 1, \dots, 9. \tag{3.10}$$

The self-energy contributes to F_1 only:

$$F_1^{self} = F_1^{D1}. \tag{3.11}$$

In a theory with several fermion flavors (with different masses m_f), one has to sum this term over all flavors. The vertices contribute to F_1 and F_5 :

$$F_1^{vert} = F_1^{D3} + F_1^{D6}, \tag{3.12}$$

$$F_5^{vert} = F_5^{D3} = F_5^{D6}, \tag{3.13}$$

with $F_1^{D6} = F_1^{D3}$. The two form factors for \mathcal{M}_5 in (3.1) are also equal but contribute to different structures there. The situation for the box diagrams is a little more involved:

$$F_j^{box} = c_b \left(F_j^{D8} + F_j^{D9} \right), \tag{3.14}$$

and the c_b will be given in (3.33). As mentioned only six of the nine form factors are independent. For the direct box diagram D8 we find the following relations:

$$F_7^{D8} = 4m^2 F_4^{D8} + 2m F_5^{D8},$$

$$\begin{aligned}
F_8^{D8} &= m^2 F_4^{D8}, \\
F_9^{D8} &= m F_4^{D8} - \frac{1}{2} F_6^{D8}.
\end{aligned} \tag{3.15}$$

There are further relations between the form factors F_j^{D8} from the direct box D8 and the F_j^{D9} of the crossed box D9:

$$\begin{aligned}
F_1^{D8} &= -F_1^{D9} + (4 - 6d) F_3^{D9}, \\
F_2^{D8} &= F_2^{D9} - (4 - 2d) F_4^{D9}, \\
F_3^{D8} &= F_3^{D9}, \\
F_4^{D8} &= -F_4^{D9}, \\
F_5^{D8} &= -2dm F_4^{D9} - F_5^{D9} + d F_6^{D9}, \\
F_6^{D8} &= F_6^{D9} - 4m F_4^{D9}, \\
F_7^{D8} &= F_7^{D9} - (4 - 2d) F_8^{D9}, \\
F_8^{D8} &= -F_8^{D9}, \\
F_9^{D8} &= F_9^{D9}.
\end{aligned} \tag{3.16}$$

Inverting relations (3.16), diagram D9 is obtained from D8 by exchanging t and u . As mentioned, the t -channel box D7 may be obtained from D8 by simply exchanging t and s (and an overall sign). Subsequently, diagram D10 results from D7 by inverting again (3.16) and exchanging now s and u . As a consistency check, one can additionally obtain D10 from D9 by s, t crossing. The inversion of the first six relations of (3.16) yields F_1^{D9} to F_6^{D9} :

$$\begin{aligned}
F_1^{D9} &= -F_1^{D8} + (4 - 6d) F_3^{D8}, \\
F_2^{D9} &= F_2^{D8} - (4 - 2d) F_4^{D8}, \\
F_3^{D9} &= F_3^{D8}, \\
F_4^{D9} &= -F_4^{D8}, \\
F_5^{D9} &= -F_5^{D8} - 2d F_9^{D8}, \\
F_6^{D9} &= -F_6^{D8} - 4 F_9^{D8}.
\end{aligned} \tag{3.17}$$

In a next step, one gets in combination with (3.15):

$$\begin{aligned}
F_7^{D9} &= -6dm^2 F_4^{D9} - 2m F_5^{D9} + 2dm F_6^{D9}, \\
F_8^{D9} &= m^2 F_4^{D9}, \\
F_9^{D9} &= m F_4^{D9} - \frac{1}{2} F_6^{D9}.
\end{aligned} \tag{3.18}$$

We see that the relations for F_7 in terms of amplitudes F_1 to F_6 are different for diagrams D8 and D9.

What remains now is to determine one form factor for the self-energy, two form factors of the vertex, and six form factors for one of the four box diagrams. This will be done in two steps. First, we collect the form factor contributions from the Feynman diagrams D1 to D10, and in a second step we have to add up additional contributions $F_j^{a,r}$ arising from counter term insertions

into the one-loop diagrams. The latter are formally of higher order, but it is reasonable to discuss them here. So, effectively, (3.10) has to be replaced by

$$F_j(s, t) = \frac{2e^2}{(4\pi)^{d/2}} \left[F_j^{\text{self}} + F_j^{\text{vert}} + F_j^{\text{box}} + \frac{\delta m}{m} \left(F_j^{\text{self},r} + F_j^{\text{vert},r} + F_j^{\text{box},r} \right) \right],$$

$$j = 1, \dots, 9. \quad (3.19)$$

Additionally, charge renormalization $\delta e/e$ will give an overall factor, and there are also contributions $F_j^Z, F_j^{Z,r}$ from wave function renormalization. Both will be discussed in Section 3.2.

3.1 The form factors

We will use the abbreviations for the five master integrals, used here and in the following for the s -channel contributions:

$$A_0 = A_0(m) \quad (3.20)$$

$$B_0 = B_0(0, 0; s) \quad (3.21)$$

$$B_t = B_0(m, m; t) \quad (3.22)$$

$$C_0 = C_0(m, 0, m; m^2, m^2, s) \quad (3.23)$$

$$C_1 = C_0(0, m, 0; m^2, m^2, s) \quad (3.24)$$

$$D_0 = D_0(m, 0, m, 0; m^2, m^2, m^2, t, s) \quad (3.25)$$

together with the function

$$C_4 = C_0(m, 0, m; m^2, m^2, t). \quad (3.26)$$

The latter may be expressed by A_0 and B_t , see (A.8). This function contains the infra-red singularities and we decided to keep it explicitley as it is also done in `LoopTools`. Further we introduce

$$w = \frac{u}{s}, \quad (3.27)$$

$$x = \frac{1}{1 - \frac{4m^2}{s}}, \quad (3.28)$$

$$y = \frac{1}{1 - \frac{4m^2}{t}}. \quad (3.29)$$

In terms of (3.20) - (3.26) the results for the amplitudes are given in the following. They may also be obtained in `FORM` format from [43]. The explicit expressions for the master integrals are discussed in Section 4. The form factors from self-energies and vertices are:

$$F_1^{\text{self}} = A_0 \frac{4}{s^2} \left[\frac{1}{d-1} - 1 \right] + B_s \frac{2}{s} \left[\frac{1}{d-1} (1-z) - 1 \right], \quad (3.30)$$

$$F_1^{\text{vert}} = 2 \left(-\frac{A_0}{m^2} \frac{1}{s} \left[\frac{1-x}{d-3} - xz \right] + B_s \frac{1}{s} [x(1+z) + d-4] \right)$$

$$-\frac{C_0}{(d-3)s}(1+x)(s-4m^2)\Big), \quad (3.31)$$

$$F_5^{\text{vert}} = A_0 \frac{2}{ms^2} x \left[\frac{2}{d-3} - (d-4) \right] + B_s \frac{4m}{s^2} x [1 - (d-4)]. \quad (3.32)$$

For the box diagrams:

$$F_j^{\text{box}} = \frac{1}{(vw)^2} (F_j^{D8} + F_j^{D9}), \quad (3.33)$$

and the six independent box form factors for that are:

$$\begin{aligned} F_1^{D8} = & v \left(A_d [2v(v_+ + 2w + vwx) + 2zw_+y] - \frac{4}{s} [B_t(w_+y + v)z + B_0vw(1 + vx)] \right. \\ & - \frac{C_4}{d-3} [(1-3z)yz^2 - v((1-6z)yz - 2(2-3z)z) - v^2(4 + (3y-10)z) - 4v^3] \\ & + C_1 v \left[\frac{1}{d-3} \{2 - z - z^2 + v(2w_+ + z)\} - 2(1-z) - 2v(1-wx) \right] \\ & - D_0 \frac{sv}{2} \left\{ \frac{1}{d-3} [-2vv_-v_+ + z(2-z-z^2) + v(1+4z)z - 5v^2z] \right. \\ & \left. \left. + 2v(1-3z+2z^2) + v^2(4-5z) + 2v^3 - (1-z)^2z \right\} \right), \end{aligned} \quad (3.34)$$

$$\begin{aligned} F_2^{D8} = & \frac{2v}{s} \left(A_d [w + 2v(1 + wx) + w_-y] - \frac{2}{s} [B_t(2v + w_-y) + B_0(1 + 2vx)w] \right. \\ & - \frac{C_4}{d-3} [y_-w_+ + v(2v - z) - z^2] \\ & + C_1 \left\{ \frac{1}{d-3} [(1-2v)(1-z) - 2v^2] - (1 + 2vxz)(1-z) \right. \\ & \left. + 2v(v(1-xz) - z) \right\} - D_0 \frac{s}{2} \left\{ \frac{1}{d-3} [(1-z)(1+w-2vz) \right. \\ & \left. - 2v^2(w+z)] + v(1 + 2v(w_+ + z) - 2z^2) \right\} \Big), \end{aligned} \quad (3.35)$$

$$F_3^{D8} = \frac{v^2w}{2} \left(-\frac{C_4}{d-3}w_+ + \frac{1}{d-3} \{C_1 - D_0 \frac{s}{2}w_+\} \right), \quad (3.36)$$

$$\begin{aligned} F_4^{D8} = & \frac{v}{s} \left(-\frac{A_d}{2} [wy_- + y] + \frac{1}{s} [B_tyw_- + B_0w] - \right. \\ & \frac{C_4}{d-3} [v^2 - \frac{v}{2}(y_- + z) - (y_- - z)(w_+ - \frac{z}{2})] - C_1 [\frac{1-z}{2} \frac{d-4}{d-3} \\ & \left. - \frac{w}{d-3} - (1-z)] + D_0 \frac{s}{4} [v - \frac{w_+}{d-3} (w + w_+ - z)] \right), \end{aligned} \quad (3.37)$$

$$F_5^{D8} = \frac{2vm}{s} \left(A_d[v + (1 + vx)w + (1 + 2w)y] - \right. \quad (3.38)$$

$$\begin{aligned} & \frac{2}{s} [B_t(v + (1 + 2w)y) + B_0(1 + vx)w] - \\ & \left. \frac{C_4}{d-3} w_+(y_- - 2wy - z) - C_1 w \left[\frac{1}{d-3} - (1 + vx_+) \right] + D_0 \frac{sw}{2} \left[\frac{w_+}{d-3} - v \right] \right), \\ F_6^{D8} &= \frac{2vm}{s} \left(A_d[v + 2wy + vwx] - \frac{2}{s} [B_t(v + 2wy) + B_0vwx] \right. \\ & \left. - \frac{C_4}{d-3} (v - z)(2v + wy) - \right. \\ & \left. C_1 v \left[\frac{1}{d-3} + x(1 + v_+ - 2z) \right] - D_0 \frac{sv}{2} \left[\frac{1}{d-3} (v - z) - 1 \right] \right), \end{aligned} \quad (3.39)$$

where we have further introduced

$$A_d = -\frac{A_0}{m^2} \frac{1}{s} \frac{d-2}{d-3}, \quad (3.40)$$

$$x_{\pm} = 1 \pm x, \quad (3.41)$$

$$y_{\pm} = 1 \pm y, \quad (3.42)$$

$$v_{\pm} = 1 \pm v, \quad (3.43)$$

$$w_{\pm} = 1 \pm w. \quad (3.44)$$

The small mass limit is easily obtained by putting $z = 0, x = y = 1$.

3.2 Counter term contributions

In this section we focus on the contributions originating from renormalization: the charge counter term, the mass counter term and the wave function renormalization are given in arbitrary dimension. Not only their $1/\epsilon$ and constant terms are needed in order to render the amplitudes from the diagrams in Fig. (3.1) finite, but also $O(\epsilon)$ terms combine with divergent parts of the unrenormalized amplitudes to give additional finite contributions. Similarly, of course, in two-loop order the $O(\epsilon)$ contributions of the diagrams combine with the $1/\epsilon$ terms of the counter terms to give finite contributions.

First we consider the charge counter term. Each diagram of Figure (3.1) has at its vertices a factor e , the electric charge. Renormalization in two-loops requires e to be replaced by $e(1 + \delta e/e)$, with the charge counter term

$$\frac{\delta e}{e} = -\frac{e^2}{(4\pi)^{d/2}} \frac{d-2}{3} \frac{A_0(m)}{m^2}. \quad (3.45)$$

While the introduction of the charge counter term results only in an overall factor, the introduction of the mass counter term is more complicated. Every internal electron propagator in Fig. 3.1 has to be replaced by:

$$\frac{1}{p_e^2 - m^2(1 + \delta m/m)^2} \simeq \frac{1}{p_e^2 - m^2} \left(1 + \frac{2m^2 \delta m/m}{p_e^2 - m^2} \right), \quad (3.46)$$

with

$$\frac{\delta m}{m} = \frac{e^2}{(4\pi)^{d/2}} \frac{(d-1)(d-2)}{2(d-3)} \frac{A_0(m^2)}{m^2}, \quad (3.47)$$

the electron mass counter-term. This means that additional amplitudes $F_j^{Dk,r}$ are obtained from the one-loop diagrams Dk : All fermion propagators are replaced according to (3.46), but the higher powers of $\delta m/m$ are dropped. The contributions from the first powers of $\delta m/m$ lead to 'dotted propagators' with squared numerators. The second recursion relation given in (A.7) reduces the resulting Feynman integrals with dotted lines to master integrals.

Since the mass renormalization counterterm $\delta m/m$ contains a $1/\epsilon$ pole, the one-loop master integrals A_0 and B_0 etc., resulting from the diagrams, are needed to order $\mathcal{O}(\epsilon)$ in order to ensure that all finite terms are taken into account properly. The relations between the nine amplitudes of a given dotted diagram fulfil similar relations as those for the undotted diagrams. The only *differences* are the following:

$$F_8^{D8,r} = m^2 F_4^{D8,r} + F_3^{D8,r}, \quad (3.48)$$

$$F_7^{D8,r} = F_7^{D9,r} - (4-2d) F_8^{D9,r} - 4 F_3^{D9,r}, \quad (3.49)$$

$$F_7^{D9,r} = -6dm^2 F_4^{D9,r} - 2m F_5^{D9,r} + 2dm F_6^{D9,r} + 2d F_3^{D9,r}, \quad (3.50)$$

$$F_8^{D9,r} = m^2 F_4^{D9,r} - F_3^{D9,r}. \quad (3.51)$$

All other relations remain unchanged.

Now we present the contributions to the amplitudes for the dotted diagrams:

$$F_1^{self,r} = A_0 \frac{4}{s^2} (d-2)xz - B_s \frac{2}{s} z [1 - (d-3)x], \quad (3.52)$$

$$\begin{aligned} F_1^{vert,r} = & 2 \left(A_0 \frac{2}{s^2} x \left[\left(\frac{-1}{d-3} + 6 \frac{1}{d-5} \right) - (d-4)(2x-1+(d-4)) + 7-4x \right] \right. \\ & + A_0 \frac{2}{m^2 s} \left[1 + 3 \frac{1}{d-5} \right] - B_s \frac{1}{s} xz [(d-4)(2x+(d-4)) + 2x] \\ & \left. + \frac{1}{(d-3)s} xz (s-4m^2) C_0 \right), \end{aligned} \quad (3.53)$$

$$\begin{aligned} F_5^{vert,r} = & -\frac{A_0}{m} \frac{4}{s^2} x \left[\frac{-1}{d-3} + (d-4) \left(1 + (d-4) \left(1 - \frac{x}{2} \right) \right) - 3 + 2x \right] - B_s \frac{4m}{s^2} x \\ & [(d-4)(x - (d-4)xz) + 2xz] - \frac{4m}{(d-3)s^2} x(1+x)(s-4m^2) C_4. \end{aligned} \quad (3.54)$$

For the box diagrams:

$$F_j^{box,r} = \frac{1}{(vw)^2} \left(F_j^{D8,r} + F_j^{D9,r} \right), \quad (3.55)$$

and the six independent dotted box form factors for that are:

$$F_1^{D8,r} = \frac{A_0}{m^2} \frac{1}{s} \left\{ (d-4) \left[2v^2(v_+(1+v_+) - xvw + 2wz) - zv \left(v(2+v_+) - wy(1+2w) \right) \right] \right.$$

$$\begin{aligned}
& +z(v+y)) - z^2 y^4 w_+ \Big] + \frac{6}{d-5} \Big[v^2(v_+(1+v_+) - vw + 2wz) + \frac{vz}{2}(v(2w-3z) \\
& + 2y(w_+^2 - w)) + \frac{v^2 z^2}{2} \Big] + 2v^2[v(4+2w_++3z) + 6(w_+^2 - w) - 2xvw] \\
& + \frac{vz}{2} \Big[w_+ - 8v(1+v_+ + \frac{3z}{4}) + y(3+17w+12w^2) \Big] + \frac{z^2}{4} [v(8v-2-4yw_-) \\
& - 4y^4(2+w)] \Big\} + A_0 \frac{2}{s^2(d-3)} \Big\{ v[y_- + w(1+9y) + 2vz - (1-2w_+y)z] \\
& + 2wy^4 z \Big\} - B_t \frac{z}{s} \Big\{ 4(d-4)[v(v+yw_+) + \frac{yz}{2}(v+yw_+)] + v(v+4v(1-z) \\
& + 5yw_- - z) + z(v+2v^2-2y(vw-y)) \Big\} - B_0 \frac{vz(d-3)}{s} \Big\{ 2v(w+w_+) \\
& + 2xvw(1+2v-z) + 2y(w^2+w_+^2) \Big\} + C_4 \frac{2}{d-3} \Big\{ v \Big[v \Big(vz(w_++v-\frac{3z}{2}) \\
& + [y_- + w(1+9y) - (5-2y+2w(2-y))z] \frac{z}{4} + \frac{z^3}{2} \Big) - [y_- + w(1+9y-2y^4)] \\
& \frac{z^2}{4} + (1-2w_+y) \frac{z^3}{4} \Big] - wy^4 \frac{z^3}{2} \Big\} + C_1 \frac{vz}{2} \Big\{ (d-4) \Big[w_+ - v(1+2w+8w^2-4v^2) \\
& + 4xv^2w + 2y(w^2+w_+^2) - z(1-4vw_++2v^2+2y(w^2+w_+^2)) - 2z^2v \Big] + \\
& - 2v(w+2vv_+-2xvw) + z(w_++(3v-z)(v+v_+)) \Big\} + D_0 vzs \Big\{ (d-4) \\
& \Big[vv_+^2 - \frac{z}{2}(v(2-2w+3v) - y(w^2+w_+^2)) + \frac{z^2}{2}v \Big] - v \Big(2 + (2v+w)w_+ + \frac{w}{2} \Big) \\
& + \frac{z}{2} \Big(v(3+2w) - y(w^2+w_+^2) \Big) \Big\}, \tag{3.56}
\end{aligned}$$

$$\begin{aligned}
F_2^{D8,r} &= \frac{A_0}{m^2 s^2} \Big\{ (d-4) \Big[2v \Big(2v(2+wx_-+z) + 4w_+y - wy_- \Big) - 2z \Big(2v(v+y) \\
& + (3+5w)y^4 \Big) \Big] - \frac{2}{d-3} vwy_- + \frac{24v}{d-5} [v+w_+y] + 2v[6v(3+v) \\
& - (3-10v+4vx-15y)w + 12y] - 2z[4v^2-2vwy+(6+9w)y^4] \Big\} \\
& + A_0 \frac{8}{s^3(d-3)} \Big\{ wy^4 + 2v(v+wy+2y) \Big\} - B_t \frac{4}{s^2} \Big\{ z(d-4) \Big[2vy + (3+5w)y^4 \Big] \\
& + vwy_- - z \Big(2v(v+yw_+) - (3+4w)y^4 \Big) \Big\} \\
& + B_0 \frac{4v}{s^2} \Big\{ (d-4)[y_- - z(1+2xvw)] + y_- - z(1+2xvw) \Big\} \\
& - C_4 \frac{2}{s(d-3)} \Big\{ v^2wy_-vz[w(1-yy_-)+2v(v+y(1+w_+))] \\
& + z^2[wy^4+2vy(2+w)+2v^2] \Big\}
\end{aligned}$$

$$\begin{aligned}
& -C_1 \frac{2v}{s} \{ (d-4)[y_- - z(1 - 2v(w_+ - xw) - y)] + 2zv(1 - wx_+) \} \\
& + D_0 v z \{ (d-4)[2vw_+ + y] - y_+ + z \}, \tag{3.57}
\end{aligned}$$

$$\begin{aligned}
F_3^{D8,r} = & -A_0 \frac{d-2}{d-3} \frac{2}{s^2} vwy - B_t \frac{1}{s} vwy z - C_4 \frac{1}{2(d-3)} vw(v-z)yz + C_1 \frac{1}{2} v^2 wz - \\
& D_0 \frac{1}{4} sv^2 wz, \tag{3.58}
\end{aligned}$$

$$\begin{aligned}
F_4^{D8,r} = & \frac{A_0}{m^2} \frac{1}{s^2} \left\{ \frac{1}{d-3} \left[-\frac{v}{2}(y_- - z) + (v - \frac{w}{2}y^3)yz \right] + \frac{3v}{d-5} [yw_+ + v] \right. \\
& + (d-4) \left[\frac{1}{2} vwy_+ + v(v+y) - \frac{1}{2} w_- y^4 z \right] \\
& + v \left[(w + \frac{z}{2})(1+2y) + \frac{7}{2}y + 3v - \frac{1}{2} \right] + \frac{1}{2} (w-2)y^4 z \Big\} \\
& + B_t \frac{1}{s^2} \left\{ \left(v(-y_- + (1+2y)z) - y^4 z \right) - (d-4)y^4 z(1+v_+ - z) \right\} \\
& - B_0 (d-3) \frac{v}{s^2} \{ y_- + 2vx(v_+ - z)(1-z) - 2v(y+v-z) - z(1-2y) \} \\
& + C_4 \frac{1}{s} \frac{1}{2(d-3)} \{ (v(1+2z) - wy^3 z)y - (1-z)v \} (v-z) \\
& - C_1 \frac{v}{s} \left\{ vz - (d-4) \left[(w + \frac{1}{2})y(1-z) + \frac{1}{2}(v-w) - vz \right] \right\} \\
& + D_0 v z \left\{ \frac{y}{4}(1-2z) + \frac{1-z}{4} + \frac{1}{2}vy_+ - (d-4) \left[\frac{y}{4}(1-2z) - \frac{v}{2}y_- \right] \right\}, \tag{3.59}
\end{aligned}$$

$$\begin{aligned}
F_5^{D8,r} = & \frac{A_0}{m} \frac{1}{s^2} \left\{ (d-4) \left[-2v(v+w+xvw+yw_+) + 2zy^4 w \right] - \frac{6v}{d-5} (yw_+ + v) + \right. \\
& 2v \left[1 - 3v - 2w - 2xvw - y(4+3w) + \frac{y_- - z}{d-3} \right] - 2z(v - 2y^4 w) \Big\} + \\
& B_t \frac{4m}{s^2} \{ vy_- + z((d-3)y^4 w - v) \} \\
& + B_0 \frac{4mv}{s^2} (d-3) [v - w + y - 2vwx(1 - \frac{z}{2})] + \\
& C_4 \frac{2vm}{s} \frac{1}{d-3} (v-z)(y_- - z) + C_1 \frac{2vm}{s} \left\{ (d-4) \left[2vw - v + w - y + z(v+y+ \right. \right. \\
& \left. \left. xvw) \right] + zxvw \right\} - D_0 2vm \left\{ \frac{z}{2} (d-4)(v+y) + vv_+ w + \frac{z}{2} [y_- - vw - z] \right\}, \tag{3.60}
\end{aligned}$$

$$F_6^{D8,r} = \frac{A_0}{m} \frac{1}{s^2} \left\{ (d-4) \left[2v(v - xvw + y) - 2zy^4 w_- \right] + \frac{6}{d-5} [v(v + yw_+)] + \right.$$

$$\begin{aligned}
& 2v(3v - 2xvw + 3y) + 2zy(2v - y(2 - w)) \Big\} - \frac{A_0}{m} \frac{2y}{s^2(d-3)} \{vw + z(wy - \\
& 2v)\} - B_t \frac{4m}{s^2} \{(d-4)zy^4w_- + yvw - zy(2v - y)\} - B_0 \frac{4m}{s^2} \{(d-3)(v(v+y) \\
& w + zxv^2w)\} - C_4 \frac{2my}{s(d-3)} \{-wyz^2 + v(w(v - y_-z) - 2(v - z)z)\} + \\
& C_1 \frac{2vm}{s} \{(d-4)[(v+y)w - z(v - w(vx - y))]\} + vw - z(2v - xvw)\} + \\
& D_0 vm \{(d-4)[z(v + yw)] + vw(v + w) + z(v(v_- - 2w) - yw) + z^2v\}. \quad (3.61)
\end{aligned}$$

Finally we investigate wave function renormalization for the electron self-energy:

$$\Sigma(p) = A(p^2) + B(p^2)(\not{p} - m). \quad (3.62)$$

The wave function renormalization is given by:

$$Z = 1 + B + 2m \frac{\partial A}{\partial p^2} \Big|_{p^2=m^2} = 1 + \delta Z, \quad (3.63)$$

and the ‘undotted’ one then reads

$$\delta Z = -\frac{e^2}{(4\pi)^{d/2}} \left\{ \frac{d-2}{2} \frac{A_0(m)}{m^2} + 4m^2 DB_0(0, m, m^2) \right\} \quad (3.64)$$

with

$$DB_0(0, m, m^2) = \frac{\partial B_0}{\partial p^2} \Big|_{p^2=m^2}. \quad (3.65)$$

The first part in (3.64) contains the UV divergence and the second the infrared divergence. Explicitly (3.65) reads

$$\begin{aligned}
DB_0(0, m, m^2) &= \frac{(d-2)}{(d-3)} \frac{1}{4m^2} \frac{A_0(m)}{m^2} \\
&= \frac{1}{(m^2)^{3-\frac{d}{2}}} \frac{\Gamma(3-\frac{d}{2})}{(d-3)(d-4)} \\
&= \frac{C_0(m, 0, m; m^2, m^2, 0)}{(d-3)}. \quad (3.66)
\end{aligned}$$

The UV divergent part of the wave function renormalization cancels the UV divergence of the vertex, and a remaining IR-singularity will be compensated by soft photon radiation. It is worth mentioning that due to (3.66) we can also write

$$\delta Z = -\frac{\delta m}{m}. \quad (3.67)$$

We now discuss the dotted diagrams. They are UV finite and the divergent contributions to the ‘dotted’ δZ come only from the IR divergence. Therefore we write the wave function renormalization from the dotted self-energy δZ^r in terms of DB_0 (or C_0 , respectively):

$$\delta Z^r = -2 \frac{e^2}{(4\pi)^{d/2}} m^2 \frac{\delta m}{m} (d-2) [6 + 4(d-4) - (d-4)^2] DB_0(0, m, m^2). \quad (3.68)$$

The resulting form factors are:

$$F_j^{Z(r)}(s, t) = \frac{4}{s} \delta Z^{(r)}. \quad (3.69)$$

The true one-loop form factors contribute to the interference with Born (as shown here explicitly) as well as to the squared one-loop correction (not shown explicitly), while the dotted form factors contribute only to the former.

4 The master integrals

The five master integrals of massive Bhabha scattering are shown in Figure 4.1. We collect here expressions for them valid in d dimensions, but also the necessary ϵ -expansions.

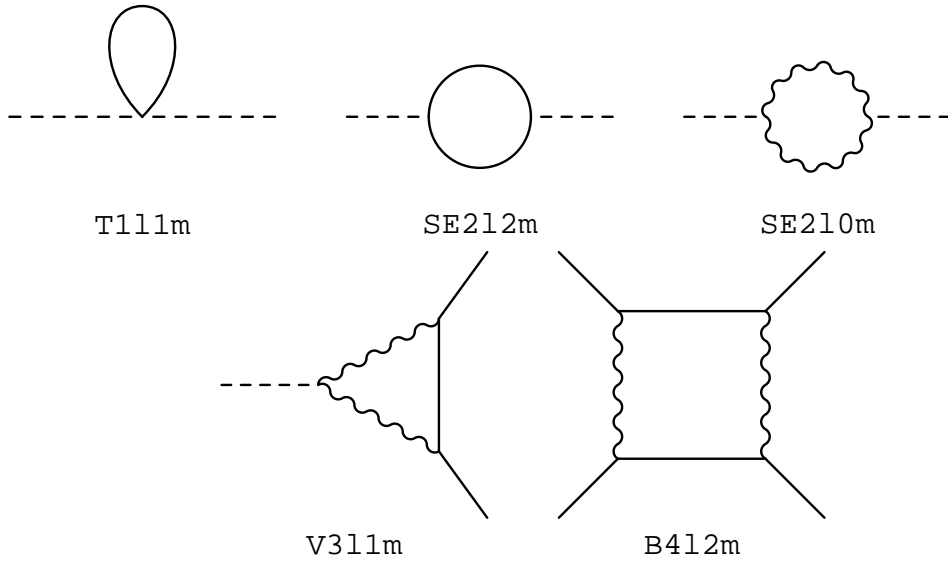


Figure 4.1: The five one-loop MIs. External solid (dashed) lines describe on- (off-)shell momenta.

4.1 One-point function

The simplest master integral is the tadpole: ²

$$\begin{aligned}
A_0(m) &= -\frac{e^{\epsilon\gamma_E}}{i\pi^{d/2}} \int \frac{d^d k}{k^2 - m^2} \\
&= \Gamma(1 - d/2)(m^2)^{\frac{d-2}{2}} \\
&= -m^2 \left[\frac{1}{\epsilon} + (1 - L_m) + \frac{\epsilon}{2} (2 + \zeta_2 - 2L_m + L_m^2) \right. \\
&\quad \left. + \frac{\epsilon^2}{6} (6 + 3\zeta_2 - 2\zeta_3 - 3(2 + \zeta_2)L_m + 3L_m^2 - L_m^3) \right] + \dots,
\end{aligned} \tag{4.1}$$

with the abbreviation

$$L_m = \ln(m^2). \tag{4.2}$$

Often, shorthand notations with $m = 1$ are used, and our tadpole formula then agrees with T111m as it is given in the Mathematica file MastersBhabha.m located at [44]:

$$\begin{aligned}
-A_0(1) &= \text{T111m} \\
&= \frac{1}{\epsilon} + 1 + \left(1 + \frac{\zeta_2}{2}\right) \epsilon + \left(1 + \frac{\zeta_2}{2} - \frac{\zeta_3}{3}\right) \epsilon^2 + \dots
\end{aligned} \tag{4.3}$$

4.2 Two-point functions

The two-point functions are

$$B_0(m, M; p^2) = \frac{e^{\epsilon\gamma_E}}{i\pi^{d/2}} \int \frac{d^d k}{(k^2 - m^2)[(k + p)^2 - M^2]}. \tag{4.4}$$

There are two of them, $B_0(0, 0; p^2)$ (coming from the reduction of box diagrams) and $B_0(m, m; p^2)$. In d dimensions, they have been determined in [45] and in [46], correspondingly:

$$B_0(0, 0; p^2) = \frac{e^{\epsilon\gamma_E} \sqrt{\pi}}{(-p^2)^{(2-\frac{d}{2})}} \frac{\Gamma(2 - \frac{d}{2}) \Gamma(\frac{d}{2} - 1)}{2^{d-3} \Gamma(\frac{d-1}{2})} \tag{4.5}$$

$$B_0(m, m; p^2) = e^{\epsilon\gamma_E} (m^2)^{-(2-\frac{d}{2})} \Gamma\left(2 - \frac{d}{2}\right) {}_2F_1\left[1, 2 - \frac{d}{2}; \frac{p^2}{4m^2}\right]. \tag{4.6}$$

The ϵ -expansion for $B_0(0, 0; p^2)$ is trivial,

$$B_0(0, 0; p^2) = \frac{1}{\epsilon} + 2 - \ln(-p^2) + \epsilon \left[4 - \frac{\zeta_2}{2} - 2 \ln(-p^2) + \frac{1}{2} \ln^2(-p^2) \right] + \dots, \tag{4.7}$$

²We omit here and in the following the conventional scale factor $(4\pi\mu^2)^\epsilon$; the scale factor would make the arguments of logarithms dimensionless.

and the one for $B_0(m, m; p^2)$ may be determined by using a relation for contiguous hypergeometric functions

$${}_2F_1\left[1, 2 - \frac{d}{2}; \frac{p^2}{4m^2}\right] = \frac{1}{1 - 2\epsilon} \left\{ 1 - 2\epsilon \left(1 - \frac{p^2}{4m^2} \right) {}_2F_1\left[1, 1 + \epsilon; \frac{p^2}{4m^2}\right] \right\}, \quad (4.8)$$

and then expanding the transformed hypergeometric function [46–49].³ The result is:

$$\begin{aligned} B_0(m, m; p^2) = & \frac{1}{\epsilon} + 2 - L_m + r \ln(x) + \epsilon \left[4 + \frac{\zeta_2}{2} - 2L_m + \frac{1}{2}L_m^2 + r \left(2 \ln(x) \right. \right. \\ & \left. \left. - \ln(x)L_m - 2 \ln(x) \ln(1+x) + \frac{1}{2} \ln^2(x) - \zeta_2 - 2\text{Li}_2(-x) \right) \right] \\ & + \epsilon^2 \left[-4L_m + L_m^2 + \zeta(2) - \frac{1}{2}\zeta(2)L_m + r \left(-2\zeta(2) + \zeta(2)L_m \right. \right. \\ & \left. \left. - 2\zeta(3) - 4\text{Li}_2(-x) + 2\text{Li}_2(-x)L_m - 2\text{Li}_3(-x) + 4S_{1,2}(-x) \right. \right. \\ & \left. \left. + 2 \ln(1+x)(\zeta(2) + 2\text{Li}_2(-x)) + 2 \ln(x) \ln^2(1+x) \right. \right. \\ & \left. \left. - (4 - 2L_m) \ln(x) \ln(1+x) - \ln(x)^2 \ln(1+x) + \frac{1}{6} \ln(x)^3 + \right. \right. \\ & \left. \left. \left(1 - \frac{1}{2}L_m \right) \ln(x)^2 + (4 - 2L_m + \frac{1}{2}L_m^2 - \frac{1}{2}\zeta(2)) \ln(x) \right) \right] + \dots, \quad (4.9) \end{aligned}$$

with

$$x = \frac{\sqrt{1 - \frac{4m^2}{p^2}} - 1}{\sqrt{1 - \frac{4m^2}{p^2}} + 1} \equiv \frac{1 - b}{1 + b}, \quad (4.10)$$

$$b = \sqrt{\frac{p^2}{p^2 - 4m^2}}, \quad (4.11)$$

$$r = \frac{1+x}{1-x} = \frac{1}{b}. \quad (4.12)$$

The ϵ -expansions may also be determined by the method of differential equations [50, 51] and are then naturally expressed in terms of Harmonic Polylogarithms [44, 52]. With $m = 1$ we have [44]:

$$\begin{aligned} B_0(0, 0; p^2) &= \text{SE210m}(x) \\ &= \frac{1}{\epsilon} + 2 + H[0, x] + 2 H[1, x] + \epsilon \left\{ (4 - \zeta_2/2 + 2 H[0, x] + 4 H[1, x] \right. \\ &\quad \left. + H[0, 0, x] + 2 (H[0, 1, x] + H[1, 0, x]) + 4 H[1, 1, x]) \right\} + \dots \quad (4.13) \end{aligned}$$

$$\begin{aligned} B_0(m, m; p^2) &= \text{SE212m}(x) \\ &= \frac{1}{\epsilon} + 2 + \frac{1+x}{1-x} H[0, x] + \epsilon \left\{ ((-8 + 8x + \zeta_2 \right. \end{aligned} \quad (4.14)$$

³We thank M. Kalmykov for the FORM code `hypergeometric2F1` for an automatized derivation of the ϵ -expansion.

$$\begin{aligned}
& +3 x \zeta_2 - 4 (1+x) H[0, x] + 4 (1+x) H[-1, 0, x] \\
& - 2 H[0, 0, x] - 2 x H[0, 0, x]) / (2 (-1+x))) \Big\} \\
& + \epsilon^2 \Big\{ ((1+x) (8 - 16/(1+x) + 3 \zeta_2 - (2 \zeta_2)/(1+x) \\
& + (5 \zeta_3)/3 + (2 \zeta_3)/(3 (1+x)) - 2 \zeta_2 H[-1, x] \\
& + ((-8 + \zeta_2) H[0, x]) / 2 + 4 H[-1, 0, x] - 2 H[0, 0, x] - 4 H[-1, -1, 0, x] \\
& + 2 H[-1, 0, 0, x] + 2 H[0, -1, 0, x] - H[0, 0, 0, x]) / (-1+x)) \Big\} + \dots
\end{aligned}$$

With the `Mathematica` file `HPL4.m.`, also located at [44], the corresponding expressions in terms of polylogarithms may be derived from (4.13) and (4.14).

4.3 Three-point functions

There are two three-point functions, $C_0(0, m, 0, m^2, m^2, p^2)$ and $C_0(m, 0, m, m^2, m^2, p^2)$, with the definition ($p = p_1 + p_2$):

$$C_0(m_1, m_2, m_3, m^2, m^2, p^2) = -\frac{e^{\epsilon\gamma_E}}{i\pi^{d/2}} \int \frac{d^d k}{[k^2 - m_1^2][(k + p_1)^2 - m_2^2][(k + p_1 + p_2)^2 - m_3^2]}. \quad (4.15)$$

As shown in (A.8) $C_0(m, 0, m, m^2, m^2, p^2)$ is not a master integral. The UV-divergences of A_0 and B_0 in (A.8) cancel, and the factor $1/(d-4)$ represents the IR-divergence of this vertex function.⁴ Due to the additional factor of $1/\epsilon$, we need A_0 and B_0 up to $O(\epsilon^2)$ for a C_0 of order ϵ . As discussed above, a separate control of IR divergences is often quite helpful in applications; therefore the explicit use of $C_0(m, 0, m; m^2, m^2, s)$ is recommended and we reproduce it here for completeness (see also Equation 39 of [46]):

$$\begin{aligned}
C_0(m, 0, m, m^2, m^2, p^2) = & \frac{-1}{(p^2 - 4m^2)b} \Big\{ \ln(x) \frac{1}{\epsilon} - \left(\ln(x) [\ln(-p^2) + \ln(-x)] \right. \\
& + 2\text{Li}_2(-x) - \frac{1}{2} \ln^2(x) + \zeta_2 \Big) + \epsilon \Big(\frac{1}{6} \ln^3(x) + \left[2\text{Li}_2(-x) \right. \\
& - \frac{1}{2} \ln^2(x) + \zeta_2 \Big] [\ln(-p^2) + \ln(-x)] + \frac{1}{2} \ln(x) [\ln(-p^2) \\
& + \ln(-x)]^2 - \frac{\zeta_2}{2} \ln(x) + 4S_{1,2}(-x) - 2\text{Li}_3(-x) - 2\zeta_3 \Big) + \dots \Big\}
\end{aligned} \quad (4.16)$$

The vertex master integral $C_0(0, m, 0, m^2, m^2, p^2)$ in d dimensions is finite for small ϵ ; it has been derived in [54]:

$$C_0(0, m, 0, m^2, m^2, p^2) = -e^{\epsilon\gamma_E} (m^2)^{\frac{d}{2}-3} \Gamma\left(2 - \frac{d}{2}\right) \left\{ \frac{1}{2(d-3)} {}_2F_1\left[\frac{1}{2}, 1; \frac{d-1}{2}; 1 - \frac{p^2}{4m^2}\right] \right\}$$

⁴The loop functions A_0 and C_0 used here deviate by an overall sign from conventions of e.g. [39, 53].

$$- \frac{\sqrt{\pi} \Gamma\left(\frac{d-2}{2}\right)}{4\Gamma\left(\frac{d-1}{2}\right)} \left(-\frac{p^2}{4m^2}\right)^{\frac{d-4}{2}} {}_2F_1\left[1, \frac{d-2}{2}; 1 - \frac{p^2}{4m^2}\right]\}. \quad (4.17)$$

Concerning the expansion with respect to ϵ , the two coefficients of the ${}_2F_1$ -functions depend on L_m and $\ln(-p^2)$, respectively. By eliminating L_m according to

$$L_m = \ln(-p^2) - (2\ln(1-x) - \ln(x)) \quad (4.18)$$

we obtain

$$\begin{aligned} C_0(0, m, 0, m^2, m^2, p^2) = & -\frac{1}{p^2 b} \left\{ \frac{1}{2} \ln^2(x) + 2\text{Li}_2(x) + 4\zeta_2 - \epsilon \left(\frac{1}{3} \ln(x)^3 - \frac{1}{2} \ln(x)^2 \right. \right. \\ & + [\ln(-p^2) - 2\ln(1+x)] \left[\frac{1}{2} \ln^2(x) + 2\text{Li}_2(x) + 4\zeta_2 \right] \\ & + \ln(x) [2\text{Li}_2(x) - 2\text{Li}_2(-x) + 5\zeta_2] - 2S_{1,2}(x^2) + 4S_{1,2}(-x) \\ & \left. \left. + 8S_{1,2}(x) + 2\text{Li}_3(-x) - 5\zeta_3 \right) \right\} + \dots \end{aligned} \quad (4.19)$$

In terms of HPLs, the function reads for $m = 1$ [44]:

$$\begin{aligned} C_0(0, m, 0, m^2, m^2, p^2) = & -\text{V311m}[\mathbf{x}] \\ = & \frac{x}{(1-x^2)} (4\zeta_2 + H[0, 0, x] + 2H[0, 1, x]) \\ & - \frac{\epsilon x}{(1-x^2)} \left[5\zeta_3 + 8\zeta_2 H[-1, x] - \zeta_2 H[0, x] + 8\zeta_2 H[1, x] \right. \\ & + 2H[-1, 0, 0, x] + 4H[-1, 0, 1, x] + H[0, 0, 0, x] \\ & + 2H[0, 0, 1, x] + 2H[0, 1, 0, x] + 4H[0, 1, 1, x] \\ & \left. + 2H[1, 0, 0, x] + 4H[1, 0, 1, x] \right]. \end{aligned} \quad (4.20)$$

4.4 Four-point function

In `LoopTools` notation [39], the four-point master integral in d dimensions with two photons in the s -channel is :

$$\begin{aligned} \text{Box}(t, s) &= D_0(m^2, m^2, m^2, m^2, t, s, m^2, 0, m^2, 0) \\ &= \frac{e^{\epsilon\gamma_E}}{i\pi^{d/2}} \int \frac{d^d k}{k^2(k^2 + 2kp_4)(k + p_1 + p_4)^2(k^2 - 2kp_3)}. \end{aligned} \quad (4.21)$$

We first give the ϵ -expansion obtained from a representation based on generalized hypergeometric functions; see Subsection 4.4.1. Here we collect and complement results presented in [54] and [55]. Given the general result for the box diagram in d dimensions, the coefficients of the ϵ -expansion are naturally obtained in terms of one-dimensional integrals. Alternatively we consider in Subsection 4.4.2 the method of differential equations, which also yields the coefficients in terms of one-dimensional integrals. These can, however, systematically be presented

in the form of generalized harmonic polylogarithms, which makes this form quite attractive if one prefers ‘analytic’ results. Finally, in Subsection 4.4.3 we add a representation in terms of a two-fold Mellin-Barnes integral, which appears to be quite elegant and has the advantage that the integrand is free of singularities even in the physical domain.

4.4.1 Hypergeometric functions

A closed expression for the box function valid in d dimensions is known from [54]. In this case a first order difference equation with respect to the dimension d was solved.⁵ Other difference equations use as parameter the powers of the propagators, see e.g. [56–58]. The general result of [54] reads:

$$\begin{aligned} e^{-\epsilon\gamma_E} \text{Box}(t, s) = & -\frac{4m^{d-4}}{s(t-4m^2)} \Gamma\left(2 - \frac{d}{2}\right) F_2\left(\frac{d-3}{2}, 1, 1, \frac{3}{2}, \frac{d-2}{2}; \frac{t}{t-4m^2}, z\right) \\ & + \frac{4m^{d-4}}{(d-3)s(t-4m^2)} \Gamma\left(2 - \frac{d}{2}\right) F_{1;1;0}^{1;2;1}\left[\begin{matrix} \frac{d-3}{2}; & \frac{d-3}{2}, 1; & 1; \\ \frac{d-1}{2}; & \frac{d-2}{2}; & -; \end{matrix} z, 1 - \frac{4m^2}{s}\right] \\ & - \frac{\sqrt{\pi}(-s)^{\frac{d-4}{2}}}{2^{d-4}m\sqrt{s}} \frac{\Gamma\left(\frac{d-2}{2}\right) \Gamma\left(2 - \frac{d}{2}\right)}{(t-4m^2)\Gamma\left(\frac{d-1}{2}\right)} F_1\left(\frac{d-3}{2}, 1, \frac{1}{2}; \frac{d-1}{2}; -\frac{u}{t-4m^2}, 1 - \frac{s}{4m^2}\right), \end{aligned} \quad (4.22)$$

with

$$z = \frac{4m^2}{s} \frac{u}{t-4m^2} > 0. \quad (4.23)$$

The two photons are in the s -channel. Naturally the cuts of the diagram are different for the t -channel case, which means that the hypergeometric functions are to be evaluated in different domains of analyticity. In (4.22), e.g., the imaginary part of the diagram comes only from the coefficient $(-s)^{(d-4)/2}$ of F_1 .

The Appell hypergeometric functions in terms of their integral representations are:

$$F_1\left(\frac{d-3}{2}, 1, \frac{1}{2}, \frac{d-1}{2}; x, y\right) = \frac{d-3}{2} \int_0^1 \frac{dt t^{\frac{d-5}{2}}}{(1-tx)\sqrt{1-ty}}, \quad (4.24)$$

$$F_2\left(\frac{d-3}{2}, 1, 1, \frac{3}{2}, \frac{d-2}{2}; x, z\right) = \int_0^1 \frac{\frac{1}{2}dt}{\sqrt{1-t}(1-tx)^{\frac{d-3}{2}}} {}_2F_1\left(1, \frac{d-3}{2}, \frac{d-2}{2}, \frac{z}{1-tx}\right), \quad (4.25)$$

and the Kampé de Fériet function is:

$$F_{1;1;0}^{1;2;1}\left[\begin{matrix} \frac{d-3}{2}; & \frac{d-3}{2}, 1; & 1; \\ \frac{d-1}{2}; & \frac{d-2}{2}; & -; \end{matrix} z, y\right] = \frac{d-3}{2} \int_0^1 \frac{dt t^{\frac{d-5}{2}}}{1-ty} {}_2F_1\left(1, \frac{d-3}{2}, \frac{d-2}{2}, zt\right). \quad (4.26)$$

⁵We just mention that in [55] also a Feynman parameter representation for D_0 was given, including terms proportional to ϵ .

See [59] for (4.24), [55] for (4.26), and (4.25) is obtained from the double integral representation of the F_2 -function [60]). With these representations we can derive the needed ϵ expansion. Due to $\Gamma(2 - \frac{d}{2})$ in the prefactors of (4.22), their ϵ -expansion has to be done up to order ϵ^2 . This can be performed by expanding the integrands. The numerical evaluation of the one-dimensional integrals of the ϵ -terms works quite nicely in general. Nevertheless partial analytic results can also be obtained, see e.g. (4.27) and (4.66). Based on [55] we also give an expansion of the integrals for the limit of small masses, i.e. $-t \gg 4m^2$ (neglecting terms of $\mathcal{O}(m^2)$ and $\mathcal{O}(m^2 \ln(m^2))$).

For the F_1 -function the ϵ -expansion is easy except for the analytic integration following the expansion. In [54] the analytic integration has been performed for an F_1 -function in which one of the arguments is $\mathcal{O}(\epsilon)$ and in [55] the corresponding transformation to obtain such a form has been described in detail. For the real part of F_1 we thus have:

$$\begin{aligned}
F_1\left(\frac{d-3}{2}, 1, \frac{1}{2}, \frac{d-1}{2}; x, y\right) = & -\frac{m}{\sqrt{sb}} \frac{d-3}{2} \left[\text{Re}\left\{ \ln(B) \right. \right. \\
& -\epsilon \left(\text{Li}_2(1-AB) + \text{Li}_2\left(1 - \frac{B}{A}\right) - 2\text{Li}_2(1-B) \right. \\
& \left. \left. + \frac{1}{2} \ln^2 A + \pi^2 \right) \right. \\
& + \epsilon^2 \left(\text{Li}_3\left(\frac{A(1-AB)}{A-B}\right) - \text{Li}_3\left(\frac{A(A-B)}{1-AB}\right) \right. \\
& + 2\text{Li}_3\left(\frac{A(1-B)}{1-AB}\right) - 2\text{Li}_3\left(\frac{A(1-B)}{A-B}\right) \\
& + 2\text{Li}_3\left(\frac{1-B}{A-B}\right) - 2\text{Li}_3\left(\frac{1-B}{1-AB}\right) \\
& + 2\left[\text{Li}_2\left(\frac{A(A-B)}{1-AB}\right) - \text{Li}_2\left(\frac{A(1-B)}{1-AB}\right) \right. \\
& \left. \left. + \text{Li}_2\left(\frac{1-B}{A-B}\right) - \text{Li}_2(-A) \right] \ln(A) \right. \\
& + \left[\frac{1}{2} \ln^2(A) - \zeta(2) \right] \ln\left(\frac{B-A}{1-AB}\right) \\
& - \frac{1}{6} \ln^3\left(\frac{B-A}{1-AB}\right) \\
& \left. \left. + \frac{1}{2} \ln(A) \ln^2\left(\frac{B-A}{1-AB}\right) \right) + \mathcal{O}(\epsilon^3) \right\} \right], \quad (4.27)
\end{aligned}$$

with

$$A = x(s) = \frac{a-1}{a+1} \sim -\frac{m^2}{s} < 0, \quad (4.28)$$

$$B = -x(t) = \frac{b-1}{b+1} \sim \frac{m^2}{t} < 0, \quad (4.29)$$

$$a = \sqrt{\frac{s - 4m^2}{s}}, \quad (4.30)$$

$$b = \sqrt{\frac{t}{t - 4m^2}}. \quad (4.31)$$

Abbreviating (4.27) as ($b \sim 1$)

$$F_1 \left(\frac{d-3}{2}, 1, \frac{1}{2}, \frac{d-1}{2}; x, y \right) = -\frac{m}{\sqrt{s}}(d-3) [F_1^0 + \epsilon F_1^1 + \epsilon^2 F_1^2], \quad (4.32)$$

we obtain from (4.27) in the limit of small masses with $r = -t/s, 0 \leq r \leq 1$:

$$\begin{aligned} F_1^0 &= -\ln\left(\frac{-t}{m^2}\right), \\ F_1^1 &= -\frac{1}{2} \ln^2\left(\frac{s}{m^2}\right) - 2\zeta(2) - \text{Li}_2\left(1 - \frac{1}{r}\right), \\ F_1^2 &= -\frac{1}{6} \ln^3\left(\frac{s}{m^2}\right) - 2\zeta(2) \ln\left(\frac{s}{m^2}\right) - \text{Li}_3\left(1 - \frac{1}{r}\right) - 2\zeta(3). \end{aligned} \quad (4.33)$$

For the F_2 - and Kampé de Fériet functions the same hypergeometric function ${}_2F_1$ needs to be expanded: ⁶

$$\begin{aligned} {}_2F_1\left(1, \frac{1}{2} - \epsilon, 1 - \epsilon, w\right) &= \frac{1}{\sqrt{1-w}} \left\{ 1 - 2\epsilon \ln(1+v) + 2\epsilon^2 [\ln^2(1+v) + \text{Li}_2(-v)] \right\} \\ &\approx \frac{1}{\sqrt{1-w}} \left\{ (1+v)^{-2\epsilon} + 2\epsilon^2 \text{Li}_2(-v) \right\} + O(\epsilon^3), \end{aligned} \quad (4.34)$$

with

$$v = \frac{1 - \sqrt{1-w}}{1 + \sqrt{1-w}}. \quad (4.35)$$

For the F_2 -function we have to use

$$w = \frac{z}{1 - xt} = \frac{4v}{(1+v)^2}, \quad (4.36)$$

and correspondingly for the Kampé de Fériet function

$$w = zt = \frac{4v}{(1+v)^2}, \quad (4.37)$$

and further in the integral (4.25)

$$\frac{(1+v)^{-2\epsilon}}{(1-tx)^{-\epsilon}} = \left(\frac{z}{4v}\right)^\epsilon, \quad (4.38)$$

⁶Again a FORM code for the automatized derivation of the ϵ -expansion by M. Kalmykov has been used.

and in the integral (4.26)

$$(t)^{-\epsilon}(1+v)^{-2\epsilon} = \left(\frac{z}{4v}\right)^\epsilon. \quad (4.39)$$

It appears natural to introduce v as integration variable. But a more precise numerical integration results from an elimination of the singularity at $t = 1$ in (4.25) by the transformation $1 - t = u^2$. We then have in the considered order for (4.25):

$$F_2\left(\frac{d-3}{2}, 1, 1, \frac{3}{2}, \frac{d-2}{2}; x, z\right) \approx \int_0^1 \frac{du}{\sqrt{xu^2 + \frac{4m^2}{s}}} \left[\left(\frac{z}{4v}\right)^\epsilon + 2\epsilon^2 \text{Li}_2(-v)\right], \quad (4.40)$$

with

$$\frac{z}{4v} = \frac{x}{4} \left(\sqrt{u^2 - \frac{4m^2}{t}} + \sqrt{u^2 + \frac{4m^2}{s} \left(1 - \frac{4m^2}{t}\right)} \right)^2 < 1, \quad (4.41)$$

and

$$v = \frac{\sqrt{u^2 - \frac{4m^2}{t}} - \sqrt{u^2 + \frac{4m^2}{s} \left(1 - \frac{4m^2}{t}\right)}}{\sqrt{u^2 - \frac{4m^2}{t}} + \sqrt{u^2 + \frac{4m^2}{s} \left(1 - \frac{4m^2}{t}\right)}} > 0. \quad (4.42)$$

For the following we write

$$F_2\left(\frac{d-3}{2}, 1, 1, \frac{3}{2}, \frac{d-2}{2}; x, z\right) = F_2^0 + \epsilon F_2^1 + \epsilon^2 F_2^2 + \dots, \quad (4.43)$$

where F_2^0 is obtained as

$$F_2^0 = \frac{1}{\sqrt{x}} \ln \left(\frac{1 + \sqrt{\frac{x}{1-z}}}{1 - \sqrt{\frac{x}{1-z}}} \right), \quad (4.44)$$

and the higher orders must be calculated from (4.40) numerically. In the limit of small electron mass they are:

$$\begin{aligned} F_2^0 &= \ln\left(\frac{s}{m^2}\right), \\ F_2^1 &= -\frac{1}{2} \ln^2\left(\frac{s}{m^2}\right) + \zeta(2) - \text{Li}_2\left(1 - \frac{1}{r}\right), \\ F_2^2 &= \frac{1}{6} \ln^3\left(\frac{s}{m^2}\right) - \ln\left(\frac{s}{m^2}\right) \left(\zeta(2) - \text{Li}_2\left(1 - \frac{1}{r}\right) \right) + \frac{1}{2} \zeta(3) + S_{1,2}\left(1 - \frac{1}{r}\right) - \text{Li}_3\left(1 - \frac{1}{r}\right). \end{aligned} \quad (4.45)$$

Similarly we perform the calculation for the Kampé de Fériet function (4.26):

$$F_{1;1;0}^{1;2;1} \left[\begin{matrix} \frac{d-3}{2}; & \frac{d-3}{2}, 1; & 1; \\ \frac{d-1}{2}; & \frac{d-2}{2}; & -; \end{matrix} \middle| z, y \right] \sim -\frac{d-3}{2} \frac{1}{\sqrt{y-z}}$$

$$\int_0^1 du \left\{ \left[\frac{1}{1+b_1 u} + \frac{1}{1-b_1 u} \right] b_1 - \left[\frac{1}{1+b_2 u} + \frac{1}{1-b_2 u} \right] b_2 \right\} \left[\left(\frac{z}{4v} \right)^\epsilon + 2\epsilon^2 \text{Li}_2(-v) \right] \quad (4.46)$$

with $v = v_0 u^2$ and

$$\begin{aligned} v_0 &= \frac{1 - \sqrt{1-z}}{1 + \sqrt{1-z}} \sim \frac{z}{4}, \quad v_1 = \frac{1 + \sqrt{1-\frac{z}{y}}}{1 - \sqrt{1-\frac{z}{y}}}, \quad v_2 = \frac{1}{v_1}, \\ b_1 &= \sqrt{\frac{v_0}{v_1}} \ll 1 \quad \text{and} \quad b_2 = \sqrt{\frac{v_0}{v_2}} = \sqrt{v_0 v_1}. \end{aligned} \quad (4.47)$$

As above for the F_2 , we formally write for the Kampé de Fériet function:

$$F_{1;1;0}^{1;2;1} \left[\begin{matrix} \frac{d-3}{2}; \frac{d-3}{2}, 1; 1; \\ \frac{d-1}{2}; \frac{d-2}{2}, -; \end{matrix} z, y \right] = \frac{d-3}{2} (K^0 + \epsilon K^1 + \epsilon^2 K^2 + \dots), \quad (4.48)$$

where K^0 is obtained as

$$K^0 = \frac{1}{b} \ln \left(\frac{(1-b_1)(1+b_2)}{(1+b_1)(1-b_2)} \right). \quad (4.49)$$

Again, investigating the small mass approximation, we have

$$\begin{aligned} K^0 &= \ln\left(\frac{s}{m^2}\right), \\ K^1 &= 3\zeta(2), \\ K^2 &= 7\zeta(3). \end{aligned} \quad (4.50)$$

Finally we see that the expansion in ϵ of the F_2 - and Kampé de Fériet functions becomes easy with the representations (4.40) and (4.46). To sum up our results, we have

$$\begin{aligned} \text{Box}(t, s) &= -\frac{2(m^2)^{-\epsilon}}{s(t-4m^2)} \Gamma(\epsilon) [F_2^0 + \epsilon F_2^1 + \epsilon^2 F_2^2 + \dots] \\ &\quad + \frac{2(m^2)^{-\epsilon}}{s(t-4m^2)} \Gamma(\epsilon) [K^0 + \epsilon K^1 + \epsilon^2 K^2 + \dots] \\ &\quad + \frac{2(\frac{-s}{4})^{-\epsilon}}{s(t-4m^2)} \Gamma(\epsilon) \frac{\Gamma(\frac{1}{2})}{\Gamma(\frac{1}{2}-\epsilon)} \Gamma(1-\epsilon) [\text{Re} \{F_1^0 + \epsilon F_1^1 + \epsilon^2 F_1^2 + \dots\}]. \end{aligned} \quad (4.51)$$

As we see, in the limit of small electron mass the $1/\epsilon$ -terms of the F_2 - and Kampé de Fériet functions cancel.

It is a very appealing fact to have the closed form of the box function as an analytical expression in d dimensions. So far, however, only partial analytic results were obtained for the terms of order ϵ , but as we observe already from (4.27), the results become quite lengthy if one prefers to present them in this form. Beyond that simple expressions in the small mass limit were obtained.

4.4.2 Harmonic polylogarithms

An alternative approach in terms of solving a differential equation for the box [61] yields in a natural manner harmonic polylogarithms. For the purpose of checking (in particular also numerically) and comparing, we repeated the calculation of [61] and shortly sketch the procedure.

To be explicit, we consider the Bhabha box diagram with two photons in the t -channel, as in [61], and the electron mass being set to 1; the analytical continuation to the s -channel is evident here. One may derive the differential operator

$$s \frac{\partial}{\partial s} = \frac{1}{2} \left\{ p_1^\mu + p_2^\mu + \frac{s}{s+t-4} (p_2^\mu - p_3^\mu) \right\} \frac{\partial}{\partial p_2^\mu} , \quad (4.52)$$

which applied to the one-loop box yields a differential equation:

$$\begin{aligned} \frac{d\text{Box}(s, t)}{ds} = & \frac{1}{2(-4+s)^2 st(-4+s+t)} \\ & \left[(-4+s)t(-2s^2 + 4(-4+t) + s(12 + (-6+d)t)) \text{Box}(x, y) \right. \\ & - 2(-4+s)(-4+d)(-4+t)t \text{V311m}(y) \\ & + 4st(-3+d) \text{SE212m}(x) \\ & - 4(-3+d)(-4+s)(-4+s+t) \text{SE210m}(y) \\ & \left. - 2(-2+d)st \text{T111m} \right], \end{aligned} \quad (4.53)$$

where

$$x = \frac{\sqrt{1-4/s}-1}{\sqrt{1-4/s}+1}, \quad (4.54)$$

$$y = \frac{\sqrt{1-4/t}-1}{\sqrt{1-4/t}+1}, \quad (4.55)$$

or

$$s = -\frac{(1-x)^2}{x}, \quad (4.56)$$

$$t = -\frac{(1-y)^2}{y}. \quad (4.57)$$

The subdiagrams T111m, SE212m, SE210m, V311m are given in the preceding sections.

Expanding now the differential equation (4.53) in ϵ and introducing the ansatz

$$\begin{aligned} \text{Box} &= \text{const B412m}(x, y) \\ &= \frac{1}{\epsilon} B_{-1} + B_0 + \epsilon B_1 + \dots, \end{aligned} \quad (4.58)$$

we may iteratively solve a system of differential equations which differ only in the inhomogeneous terms:

$$\frac{dB_j(x, y)}{dx} = \frac{1 + x^2}{x(1 - x^2)} B_j(x, y) + C_j(x, y). \quad (4.59)$$

More details are described in the literature, e.g. in [61].

The result is

$$B_{-1} = \frac{2xyH(0, x)}{(1 - x^2)(1 - y)^2} = \frac{2}{st\sqrt{1 - 4/s}} H(0, x), \quad (4.60)$$

where $H(0, x) \equiv \ln(x)$ has been introduced,

$$B_0 = \frac{2}{st\sqrt{1 - 4/s}} H(0, x) \left(H(0, y) + 2H(1, y) \right), \quad (4.61)$$

and finally

$$\begin{aligned} B_1 = & \frac{-2}{st\sqrt{1 - 4/s}} \left\{ G\left(-\frac{1}{y}, 0, 0, x\right) + G(-y, 0, 0, x) \right. \\ & - 2\left(G\left(-\frac{1}{y}, -1, 0, x\right) + G(-y, -1, 0, x)\right) \\ & - \left(G\left(-\frac{1}{y}, 0, x\right) + G(-y, 0, x) - 2H(-1, 0, x)\right) [H(0, y) + 2H(1, y)] \\ & - \left(G\left(-\frac{1}{y}, x\right) - G(-y, x) + H(0, x)\right) [H(0, 0, y) + 2H(0, 1, y)] \\ & - \left(5G\left(-\frac{1}{y}, x\right) - 3G(-y, x) - \frac{1}{2}H(0, x) - 2H(-1, x) - 4H(0, y)\right) \zeta_2 \\ & - 2\left(H(1, y)H(0, 0, y) - H(0, y)H(0, 1, y)\right) \\ & - 2\left(H(-1, 0, 0, x) - 2H(-1, -1, 0, x)\right) - 2H(0, x)[H(1, 0, y) + 2H(1, 1, y)] \\ & \left. + H(0, 0, 0, y) + 2H(1, 0, 0, y) - 2\zeta_3 \right\}. \end{aligned} \quad (4.62)$$

The functions G are generalized harmonic polylogarithms [61, 62]. For the calculation of B_1 we used the relations

$$G(-y, 0, 0, 1) = -\zeta_2 H(0, y) + H(0, 0, -1, y) - H(0, 0, 0, y), \quad (4.63)$$

$$G(-y, -1, 0, 1) + G\left(-\frac{1}{y}, -1, 0, 1\right) = -\frac{3}{2}\zeta_3 - \zeta_2 H(-1, y) + H(1, 0, 0, y) + H(0, 0, -1, y). \quad (4.64)$$

There is a difference in the coefficient of the term $H(0, x)\zeta_2$ w.r.t. [61] due to different choices of normalization, see also (4.60).

In order to check the results, we evaluated both representations of B_1 numerically (for the photons in the s -channel). For $s = 10^6$, $\cos \theta = 0.4$, $m = 1$, agreement to nine decimals was achieved:

$$B_1(s = 10^6, \cos \theta = 0.4) = 4.43779985 \cdot 10^{-9} - 1.61529999 \cdot 10^{-9} i. \quad (4.65)$$

The most difficult part of the numerical evaluation of (4.62) is the calculation of $G(-y, -1, 0, x)$, in which case a principal value integral has to be performed with the above parameters. The imaginary part obtained from (4.62) therefore agrees only to 7 decimals with (4.65). Following [55], a simple formula for the imaginary part of B_1 can be derived, which is indeed simpler than what is obtained from (4.62):

$$\begin{aligned} \Im(B_1) = & \frac{\pi}{s\sqrt{t(t-4)}} \\ & \left(2\text{Li}_2(1+xy) + 2\text{Li}_2(1+y/x) + 4\text{Li}_2(-y) + \ln^2(-x) + \frac{\pi^2}{3} \right. \\ & \left. + 2\ln(y)[\ln(s) + 2\ln(1+y)] \right). \end{aligned} \quad (4.66)$$

This yields the imaginary part of the above number. The numerical calculations were performed with *Mathematica* and *Maple*, respectively.

4.4.3 Mellin-Barnes representation

Finally, we derive a Mellin-Barnes representation for the QED box integral, again with two photons in the s -channel. The Mellin-Barnes representation reads for finite ϵ :

$$\begin{aligned} \text{Box}(t, s) = & \frac{e^{\epsilon\gamma_E}}{\Gamma[-2\epsilon](-t)^{(2+\epsilon)}} \frac{1}{(2\pi i)^2} \int_{-i\infty}^{+i\infty} dz_1 \int_{-i\infty}^{+i\infty} dz_2 \\ & \frac{(-s)^{z_1} (m^2)^{z_2}}{(-t)^{z_1+z_2}} \Gamma[2+\epsilon+z_1+z_2] \Gamma^2[1+z_1] \Gamma[-z_1] \Gamma[-z_2] \\ & \Gamma^2[-1-\epsilon-z_1-z_2] \frac{\Gamma[-2-2\epsilon-2z_1]}{\Gamma[-2-2\epsilon-2z_1-2z_2]} \end{aligned} \quad (4.67)$$

A derivation may be found e.g. in [63]. Starting from this Mellin-Barnes integral, one has to perform an analytic continuation in ϵ from a domain where the integral is regular into the vicinity of the origin. The singularity structure near $\epsilon \sim 0$ is obtained by means of the *Mathematica* package MB [64]. We obtain the result in terms of the following one- and two-dimensional integrals:

$$\text{I1} = \frac{e^{\epsilon\gamma_E}}{st} \frac{1}{2\pi i} \int_{-\frac{1}{2}-i\infty}^{-\frac{1}{2}+i\infty} dz_1 \left(\frac{m^2}{-t} \right)^{z_1} \frac{\Gamma^3[-z_1] \Gamma[1+z_1]}{\Gamma[-2z_1]}, \quad (4.68)$$

and

$$\text{I2} = \frac{e^{\epsilon\gamma_E}}{t^2} \frac{1}{(2\pi i)^2} \int_{-\frac{3}{4}-i\infty}^{-\frac{3}{4}+i\infty} dz_1 \left(\frac{-s}{-t} \right)^{z_1} \Gamma[-z_1] \Gamma[-2(1+z_1)] \Gamma^2[1+z_1] \quad (4.69)$$

$$\times \int_{-\frac{1}{2}-i\infty}^{-\frac{1}{2}+i\infty} dz_2 \left(\frac{m^2}{-t} \right)^{z_2} \Gamma[-z_2] \frac{\Gamma^2[-1-z_1-z_2]}{\Gamma[-2(1+z_1+z_2)]} \Gamma[2+z_1+z_2].$$

In terms of the conformally mapped variable

$$y = \frac{\sqrt{1-4m^2/t}-1}{\sqrt{1-4m^2/t}+1}, \quad (4.70)$$

the first integral $\mathbb{I}1$ in (4.68) can be performed analytically to yield the well known result

$$\mathbb{I}1 = \frac{1}{m^2 s} \frac{2y}{1-y^2} \ln(y). \quad (4.71)$$

The final result for the Box then reads:

$$\text{Box}(t, s) = -\frac{1}{\epsilon} \mathbb{I}1 + \ln(-s) \mathbb{I}1 + \epsilon \left(\frac{1}{2} [\zeta(2) - \ln^2(-s)] \mathbb{I}1 - 2\mathbb{I}2 \right). \quad (4.72)$$

The first two terms are in evident agreement with (4.60) and (4.61). The double integral $\mathbb{I}2$ in (4.70) is not easily evaluated analytically, although we know the answer from (4.62). The MB package yields fairly precise values in the Euclidean region ($s < 0$). In the Minkowskian domain (with $s > 0$ and $(-s)^{z_1} = s^{z_1} \exp(-i\pi z_1)$) our experience with Mathematica is that the built-in function `NIntegrate` with `MaxRecursion` \rightarrow 12 gives easily a precision of nine decimals. An alternative is the expansion at small m and fixed value of t . With

$$m_t = \frac{-m^2}{t}, \quad (4.73)$$

$$r = \frac{s}{t}, \quad (4.74)$$

we have obtained a compact answer for $\mathbb{I}2$ with the additional aid of XSUMMER [65]. The box contribution in this limit becomes:

$$\begin{aligned} B_1 = \frac{1}{st} & \left\{ 4\zeta_3 - 9\zeta_2 \ln(m_t) + \frac{2}{3} \ln^3(m_t) + 6\zeta_2 \ln(r) - \ln^2(m_t) \ln(r) \right. \\ & + \frac{1}{3} \ln^3(r) - 6\zeta_2 \ln(1+r) + 2\ln(-r) \ln(r) \ln(1+r) - \ln^2(r) \ln(1+r) \\ & \left. + 2\ln(r) \text{Li}_2(1+r) + 2\text{Li}_3(-r) \right\} + \mathcal{O}(m_t). \end{aligned} \quad (4.75)$$

5 Summary

A calculation of Bhabha scattering for the luminosity measurement at ILC is promoted by several groups, aiming at a precision of 0.01%. With this study, we provide a publicly available program for the one-loop electroweak Standard Model corrections. Further we collect all needed expressions for the factorizing one-loop QED corrections. They are necessary ingredients for the full two-loop calculation of Bhabha scattering.

Acknowledgements

We would like to thank O. Tarasov and A. Werthenbach for cooperation at an early stage of the project and M. Kalmykov for discussions, some checks, and his FORM code for the ϵ -expansion of hypergeometric functions prior to publication. J.F. is grateful to DESY, Zeuthen for support.

A Reduction of tensor and scalar loop functions to master integrals

We strictly apply here dimensional regularization, i.e. infrared as well as ultraviolet singularities are given in terms of only one pole in $\epsilon = (4 - d)/2$.

After using DIANA [36] and FORM 3.1 in order to express the Feynman diagrams in terms of tensor integrals, we have to express the latter ones by scalar integrals: writing the m^{th} scalar amplitude of a diagram formally as

$$F_m^{Diagram} = \sum_{n,l} I_{n,l}^0 + \sum_{i,n,l} p_{i,\mu} I_{n,l}^\mu + \sum_{i,j,n,l} p_{i,\mu} p_{j,\nu} I_{n,l}^{\mu\nu} \quad (A.1)$$

where momenta $p_{i,\mu}$ are the ‘chords’, i.e. momenta in the propagators $c_i = (k - p_i)^2 - m_i^2$, with k the loop momentum. The generically denoted n -point scalar, vector, and tensor integrals $I_{n,l}^0, I_{n,l}^\mu, I_{n,l}^{\mu,\nu}$ will be transformed into scalar integrals with shifted space-time dimension d , which are then reduced to scalar integrals in generic dimension by means of recursion relations [66–68]. The indices l in (A.1) stand for ‘dots’ on lines l . The reduction to scalar integrals reads:

$$\begin{aligned} I_{n,j}^\mu &= \int^d k_\mu \prod_{r=1}^n c_r^{-(1+\delta_{rj})} = - \sum_{i=1}^{n-1} p_i^\mu n_{ij} I_{n,ij}^{[d+]}, \\ I_{n,l}^{\mu\nu} &= \int^d k_\mu k_\nu \prod_{r=1}^n c_r^{-(1+\delta_{rl})} = \sum_{i,j=1}^{n-1} p_i^\mu p_j^\nu n_{ijl} I_{n,ijl}^{[d+]^2} - \frac{1}{2} g^{\mu\nu} I_{n,l}^{[d+]}, \end{aligned} \quad (A.2)$$

where $[d+]$ is an operator shifting the space-time dimension by two units, $n_{ij} = (1+\delta_{ij})!$, $n_{ijl} = (1 + \delta_{ij} + \delta_{il} + \delta_{jl} - \delta_{ij}\delta_{il}\delta_{jl})!$ and

$$I_{n,ij\dots} = \int^d \prod_{r=1}^n \frac{1}{c_r^{1+\delta_{ri}+\delta_{rj}+\dots}}, \quad \int^d \equiv \int \frac{d^d k}{\pi^{d/2}} \quad (A.3)$$

is the original scalar integral with additional powers (dots) of the i -th and j -th propagators. The case with no dots is formally obtained by putting $j = l = 0$. Having reduced the tensor integrals to scalar integrals, the generic space-time dimension d needs to be re-established and the dots to be removed. For this we use the recurrence relations first proposed in [67], which are complementary to those obtained via integration by parts [69, 70], and later simplified and

extended to zero Gram determinants in [68]. With $Y_{ij} = -(p_i - p_j)^2 + m_i^2 + m_j^2$ and the Cayley determinant

$$()_n \equiv \begin{vmatrix} 0 & 1 & 1 & \dots & 1 \\ 1 & Y_{11} & Y_{12} & \dots & Y_{1n} \\ 1 & Y_{12} & Y_{22} & \dots & Y_{2n} \\ \vdots & \vdots & \vdots & \ddots & \vdots \\ 1 & Y_{1n} & Y_{2n} & \dots & Y_{nn} \end{vmatrix}, \quad (\text{A.4})$$

the so-called signed minors $\binom{j_1 j_2 \dots}{i_1 i_2 \dots}_n$ are determinants where the rows j_1, j_2, \dots and columns i_1, i_2, \dots are erased from the Cayley determinant $()_n$.⁷ Making successive use of the following three recurrence relations leads to scalar master integrals A_0, B_0, C_0 and D_0 in d dimensions:

$$()_n \nu_j \mathbf{j}^+ I_n^{(d+2)} = \left[-\binom{j}{0}_n + \sum_{k=1}^n \binom{j}{k}_n \mathbf{k}^- \right] I_n^{(d)}, \quad (\text{A.5})$$

$$\begin{aligned} \binom{0}{0}_n \nu_j \mathbf{j}^+ I_n^{(d)} &= \left[\left(1 + \sum_{i=1}^n \nu_i - d \right) \binom{0}{j}_n - \sum_{k=1}^n \binom{0j}{0k}_n (\nu_k - 1) \right] I_n^{(d)} \\ &\quad - \sum_{i,k \atop i \neq k}^n \binom{0j}{0k}_n \nu_i \mathbf{k}^- \mathbf{i}^+ I_n^{(d)}, \end{aligned} \quad (\text{A.6})$$

$$(d - \sum_{i=1}^n \nu_i + 1) ()_n I_n^{(d+2)} = \left[\binom{0}{0}_n - \sum_{k=1}^n \binom{0}{k}_n \mathbf{k}^- \right] I_n^{(d)}. \quad (\text{A.7})$$

These relations are applied in a FORM program one after the other: the (A.5) reduces the dimension and the index of the j^{th} line, the (A.6) reduces the index of the j^{th} line without changing the space-time dimension. The third relation (A.7) also reduces the space-time. The operators $\mathbf{i}^+, \mathbf{j}^+$ raise the power of the corresponding propagator by one unit, while \mathbf{k}^- reduces the power of the k -th propagator by one unit.

For Bhabha scattering in particular there is one subtlety: there occur zero Gram determinants and for this case special care must be taken. The occurrence of zero Gram determinants (e.g. $()_n = 0$) is discussed in [68]. Effectively a zero Gram determinant reflects the kinematical boundaries of phase space where a given n -point function can be expressed through scalar integrals of lower rank. A typical example of such simplifications is

$$C_0(m, 0, m; m^2, m^2, s) = \frac{1}{s - 4m^2} \left[\frac{d-2}{d-4} \frac{A_0(m^2)}{m^2} + \frac{2d-3}{d-4} B_0(m, m; s) \right]. \quad (\text{A.8})$$

(A.8) means that this C_0 is strictly speaking not a master integral. For practical reasons, however, we include it in the list of master integrals: see the discussion in Section 4.3. It is instructive to derive (A.8) in order to demonstrate how the procedure works. Setting the momenta of the

⁷Note here the additional overall sign $(-1)^{j_1+j_2+\dots+i_1+i_2+\dots}$.

incoming massive lines to p_1 and p_2 (the third momentum $q = -p_1 - p_2$, $q^2 = s$) and the integration momentum on the massless line (no. 3), then the chords are, respectively, $-p_1, p_2$ and 0. Correspondingly we have for the Cayley determinant

$$()_3 \equiv \begin{vmatrix} 0 & 1 & 1 & 1 \\ 1 & 2m^2 & -s + 2m^2 & 0 \\ 1 & -s + 2m^2 & 2m^2 & 0 \\ 1 & 0 & 0 & 0 \end{vmatrix} = s(s - 4m^2), \quad (\text{A.9})$$

Apparently $\binom{0}{0}_3 = 0$. Applying (A.7) with $d \rightarrow d - 2$, we obtain

$$(d - 4) ()_3 I_3^d = - \sum_{k=1}^3 \binom{0}{k}_3 \mathbf{k}^- I_3^{(d-2)}, \quad (\text{A.10})$$

where $\binom{0}{1}_3 = \binom{0}{2}_3 = 0$ and $\binom{0}{3}_3 = -s(s - 4m^2)$.

Now we have expressed our three point function already in terms of a two point function with two massive lines, however in $d - 2$ dimensions, i.e.

$$(d - 4) I_3^d = \mathbf{3}^- I_3^{(d-2)} \quad (\text{A.11})$$

and we must increase the dimension again with the intention to obtain an integral with nonvanishing Gram determinant. The relevant relation to be used is (29) in [68]

$$\sum_{j=1}^n \nu_j \mathbf{j}^+ I_n^{(d+2)} = -I_n^d, \quad (\text{A.12})$$

which in our case yields

$$I_2^{(d-2)} = - \sum_{j=1}^2 \mathbf{j}^+ I_2^d = -2 \mathbf{1}^+ I_2^d, \quad (\text{A.13})$$

i.e. a two point function in generic dimension with a dot on one of the two massive lines and we have to remove the dot from the line. In this case we have $()_2 = -2s$ and $\binom{0}{0}_2 = -s(s - 4m^2)$, i.e. both Gram determinants are nonvanishing and we can apply (A.6), which yields straightforwardly (A.8).

References

- [1] H. Bhabha, *Proc. Roy. Soc.* **A154** (1936) 195.
- [2] M. Consoli, *Nucl. Phys.* **B160** (1979) 208.
- [3] M. Böhm, A. Denner, W. Hollik, and R. Sommer, *Phys. Lett.* **B144** (1984) 414.
- [4] K. Tobimatsu and Y. Shimizu, *Prog. Theor. Phys.* **75** (1986) 905.

- [5] M. Böhm, A. Denner, and W. Hollik, *Nucl. Phys.* **B304** (1988) 687.
- [6] S. Kuroda, T. Kamitani, K. Tobimatsu, S. Kawabata, and Y. Shimizu, *Comput. Phys. Commun.* **48** (1988) 335–351.
- [7] D. Bardin, W. Hollik, and T. Riemann, *Z. Phys.* **C49** (1991) 485–490.
- [8] W. Beenakker, F. Berends, and S. van der Marck, *Nucl. Phys.* **B349** (1991) 323–368.
- [9] G. Montagna, F. Piccinini, O. Nicrosini, G. Passarino, and R. Pittau, *Nucl. Phys.* **B401** (1993) 3–66.
- [10] J. Field and T. Riemann, *Comput. Phys. Commun.* **94** (1996) 53–87, hep-ph/9507401.
- [11] W. Beenakker and G. Passarino, *Phys. Lett.* **B425** (1998) 199–207, hep-ph/9710376.
- [12] J. Küblbeck, M. Böhm, and A. Denner, *Comput. Phys. Commun.* **60** (1990) 165–180.
- [13] T. Hahn, *Comput. Phys. Commun.* **140** (2001) 418–431, hep-ph/0012260.
- [14] G. Belanger *et al.*, hep-ph/0308080.
- [15] A. Lorca and T. Riemann, *Comput. Phys. Commun.* **174** (2006) 71–82, hep-ph/0412047.
- [16] S. Jadach, W. Placzek, E. Richter-Was, B. Ward, and Z. Was, *Comput. Phys. Commun.* **102** (1997) 229–251.
- [17] M. Melles, *Acta Phys. Polon.* **B28** (1997) 1159–1206, hep-ph/9612348.
- [18] A. Arbuzov *et al.*, *Nucl. Phys.* **B485** (1997) 457–502, hep-ph/9512344.
- [19] A. Arbuzov *et al.*, *Nucl. Phys. Proc. Suppl.* **51C** (1996) 154–163, hep-ph/9607228.
- [20] A. Arbuzov, hep-ph/9907298.
- [21] Two Fermion Working Group Collaboration, M. Kobel *et al.*, hep-ph/0007180.
- [22] S. Jadach, hep-ph/0306083.
- [23] ECFA/DESY LC Physics Working Group Collaboration, J. Aguilar-Saavedra *et al.*, DESY 2001–01 (2001), hep-ph/0106315.
- [24] Z. Bern, L. Dixon, and A. Ghinculov, *Phys. Rev.* **D63** (2001) 053007, hep-ph/0010075.
- [25] R. Bonciani, A. Ferroglia, P. Mastrolia, E. Remiddi, and J. van der Bij, *Nucl. Phys.* **B701** (2004) 121–179, hep-ph/0405275.
- [26] M. Czakon, J. Gluza and T. Riemann, *Nucl. Phys. Proc. Suppl.* **135** (2004) 83, hep-ph/0406203.

- [27] M. Czakon, J. Gluza, and T. Riemann, *Phys. Rev.* **D71** (2005) 073009, hep-ph/0412164.
- [28] A. Penin, *Phys. Rev. Lett.* **95** (2005) 010408, hep-ph/0501120.
- [29] R. Bonciani and A. Ferroglia, *Phys. Rev.* **D72** (2005) 056004, hep-ph/0507047.
- [30] J. Körner, Z. Merebashvili, and M. Rogal, *Phys. Rev.* **D71** (2005) 054028, hep-ph/0412088.
- [31] J. Körner, Z. Merebashvili, and M. Rogal, *Phys. Rev.* **D73** (2006) 034030, hep-ph/0511264.
- [32] J. Fleischer, A. Lorca, and T. Riemann, hep-ph/0409034.
- [33] A. Lorca and T. Riemann, *Nucl. Phys. Proc. Suppl.* **135** (2004) 328, hep-ph/0407149.
- [34] J. Gluza, A. Lorca, and T. Riemann, *Nucl. Instrum. Meth.* **534** (2004) 289, hep-ph/0409011.
- [35] A. Lorca, DESY-THESIS-2005-004 (2005).
- [36] M. Tentyukov and J. Fleischer, *Comput. Phys. Commun.* **132** (2000) 124–141, hep-ph/9904258.
- [37] P. Nogueira, *J. Comput. Phys.* **105** (1993) 279.
- [38] J. Vermaseren, math-ph/0010025.
- [39] T. Hahn and M. Pérez-Victoria, *Comput. Phys. Commun.* **118** (1999) 153, hep-ph/9807565.
- [40] G. J. van Oldenborgh, *Comput. Phys. Commun.* **66** (1991) 1.
- [41] W. Beenakker and A. Denner, *Nucl. Phys.* **B338** (1990) 349–370.
- [42] J. Fleischer, A. Leike, T. Riemann, and A. Werthenbach, *Eur. Phys. J.* **C31** (2003) 37, hep-ph/0302259.
- [43] T. Riemann *et al.*, <http://www-zeuthen.desy.de/theory/research/bhabha/bhabha1.html>.
- [44] M. Czakon, J. Gluza, and T. Riemann, <http://www-zeuthen.desy.de/theory/research/bhabha/bhabha.html>.
- [45] G. 't Hooft and M. Veltman, *Nucl. Phys.* **B44** (1972) 189–213.
- [46] A. Davydychev and M. Kalmykov, *Nucl. Phys.* **B605** (2001) 266–318, hep-th/0012189.
- [47] A. Davydychev and M. Kalmykov, *Nucl. Phys.* **B699** (2004) 3, hep-th/0303162.
- [48] M. Kalmykov, *JHEP* **0604** (2006) 056, hep-th/0602028.
- [49] M. Kalmykov, <http://theor.jinr.ru/~kalmykov/>.
- [50] A. Kotikov, *Phys. Lett.* **B259** (1991) 314–322.

- [51] E. Remiddi, *Nuovo Cim.* **A110** (1997) 1435–1452, hep-th/9711188.
- [52] E. Remiddi and J. Vermaseren, *Int. J. Mod. Phys.* **A15** (2000) 725–754, hep-ph/9905237.
- [53] T. Hahn, The LoopTools Homepage, <http://www.feynarts.de/looptools/>.
- [54] J. Fleischer, F. Jegerlehner, and O. Tarasov, *Nucl. Phys.* **B672** (2003) 303–328, hep-ph/0307113.
- [55] J. Fleischer, T. Riemann, and O. Tarasov, *Acta Phys. Polon.* **B34** (2003) 5345–5356.
- [56] S. Laporta, *Phys. Lett.* **B504** (2001) 188–194, hep-ph/0102032.
- [57] S. Laporta, *Int. J. Mod. Phys.* **A15** (2000) 5087–5159, hep-ph/0102033.
- [58] S. Laporta, hep-ph/0311065.
- [59] Wolfram Research, <http://mathworld.wolfram.com>.
- [60] A. Prudnikov, Y. Brychkov, and O. Marichev, *Integrals and Series, Vol. 3: More Special Functions*. Nauka, Moskva, 1986.
- [61] R. Bonciani, A. Ferroglia, P. Mastrolia, E. Remiddi, and J. van der Bij, *Nucl. Phys.* **B681** (2004) 261–291, hep-ph/0310333.
- [62] T. Gehrmann and E. Remiddi, *Nucl. Phys.* **B601** (2001) 248–286, hep-ph/0008287.
- [63] V. Smirnov, “Evaluating Feynman Integrals” (Springer Verlag, Berlin, 2004).
- [64] M. Czakon, hep-ph/0511200.
- [65] S. Moch and P. Uwer, *Comput. Phys. Commun.* **174** (2006) 759–770, math-ph/0508008.
- [66] A. Davydychev, *Phys. Lett.* **B263** (1991) 107–111.
- [67] O. Tarasov, *Phys. Rev.* **D54** (1996) 6479–6490, hep-th/9606018.
- [68] J. Fleischer, F. Jegerlehner, and O. V. Tarasov, *Nucl. Phys.* **B566** (2000) 423–440, hep-ph/9907327.
- [69] F. Tkachov, *Phys. Lett.* **B100** (1981) 65–68.
- [70] K. Chetyrkin and F. Tkachov, *Nucl. Phys.* **B192** (1981) 159–204.